Published in final edited form as:
J Geophys Res. 2010 March 24; 115: C03021. doi:10.1029/2009JC005283.

Processes influencing seasonal hypoxia in the northern California Current System

T. P. Connolly[1], **B. M. Hickey**[1], **S. L. Geier**[1], and **W. P. Cochlan**[2]

[1] University of Washington, School of Oceanography, Seattle, WA, USA

[2] Romberg Tiburon Center for Environmental Studies, San Francisco State University, Tiburon, CA, USA

Abstract

This paper delineates the role of physical and biological processes contributing to hypoxia, dissolved oxygen (DO) < 1.4 mL/L, over the continental shelf of Washington State in the northern portion of the California Current System (CCS). In the historical record (1950–1986) during the summer upwelling season, hypoxia is more prevalent and severe off Washington than further south off northern Oregon. Recent data (2003–2005) show that hypoxia over the Washington shelf occurred at levels previously observed in the historical data. 2006 was an exception, with hypoxia covering ~5000 km^2 of the Washington continental shelf and DO concentrations below 0.5 mL/L at the inner shelf, lower than any known previous observations at that location. In the four years studied, upwelling of low DO water and changes in source water contribute to interannual variability, but cannot account for seasonal decreases below hypoxic concentrations. Deficits of DO along salinity surfaces, indicating biochemical consumption of DO, vary significantly between surveys, accounting for additional decreases of 0.5–2.5 mL/L by late summer. DO consumption is associated with denitrification, an indicator of biochemical sediment processes. Mass balances of DO and nitrate show that biochemical processes in the water column and sediments each contribute ~50% to the total consumption of DO in near-bottom water. At shorter than seasonal time scales on the inner shelf, along-shelf advection of hypoxic patches and cross-shelf advection of seasonal gradients are both shown to be important, changing DO concentrations by 1.5 mL/L or more over five days.

Index terms

Hypoxic environments; Continental shelf and slope processes; Eastern boundary currents; Physical and biogeochemical interactions; Climate and interannual variability

1. Introduction

Recent time series studies in the Northeast Pacific have found long-term decreases in dissolved oxygen (DO) at oceanic and neritic locations [Whitney et al., 2007; Bograd et al., 2008]. Such a broad-scale trend could intensify impacts of low DO (or “hypoxic”) events in the northern California Current system, particularly over the inner continental shelf [Grantham et al., 2004; Chan et al., 2008]. Coastal upwelling regions along eastern boundaries like the California Current system (CCS) receive high inputs of nutrients from depth and are characterized by high rates of primary productivity [Ryther, 1969; Pauly and Christensen, 1995]. Organic matter degradation in the water column and sediments consumes DO in near-bottom water, but

Corresponding author address: Thomas P. Connolly, University of Washington, Ocean Sciences Building, School of Oceanography, Box 355351, Seattle, WA 98195-5351, tompc@u.washington.edu, (206) 543-8543.

differences in near-bottom DO concentrations between different regions, and between seasons, can also be influenced by physical processes. Before long term impacts can be adequately modeled and even predicted, it is necessary to understand past conditions and the processes that contribute to hypoxia.

In this paper, historical data (1950–1986) are used to describe local and regional patterns in the timing and severity of hypoxia off the coasts of Washington and Oregon. Recent interdisciplinary survey data from the Washington shelf (2003–2006) are used to assess the relative contributions of seasonal upwelling, interannual source water variability and biochemical consumption of DO in both the water column and sediments. The importance of along-shelf and cross-shelf advection in response to wind events over the inner shelf is assessed using data from moored sensors.

The continental shelf of Washington (Fig. 1) is located in the northern CCS. The seasonal cycle of upwelling favorable wind stress peaks in summer, though downwelling and relaxation events still occur throughout this season [Hickey, 1979;Hickey, 1998]. During the annual spring transition, oceanographic conditions change over the course of several days to weeks from the mean winter state of predominantly poleward flow and level isopycnals to the mean summer state of predominantly equatorward flow and isopycnals that tilt upward towards the coast [Strub et al., 1987]. Previous studies have shown that, like all other water properties, DO concentrations exhibit strong seasonality in this region [Landry et al., 1989]. Seasonal minima in subsurface DO concentrations over the Washington and Oregon shelves, in the bottom depth range 70–130 m, are coincident with denser water and high macro-nutrients. The permanent oxygen minimum zone in the North Pacific, where pelagic DO concentrations fall below 0.5 mL/L, intersects the slope between depths of ~600–1300 m [Sverdrup et al., 1942], well below the source of upwelled water. Though dissolved oxygen concentrations have been related to hypoxia on the Oregon shelf [Grantham et al., 2004;Hales et al., 2006;Chan et al, 2008], previous descriptions of DO concentrations on the Washington shelf have not discussed hypoxia.

The magnitude and direction of coastal currents vary with distance from shore and depth from the bottom. A baroclinic equatorward coastal jet is present over the shelf throughout the summer and the poleward California Undercurrent develops at the shelf break and slope during late summer to early fall [Hickey, 1979; Hickey, 1989]. The California Undercurrent is characterized by relatively warm, high salinity, low DO equatorial water [Hickey, 1979; Lynn and Simpson, 1987]. Over the inner shelf, the surface and bottom Ekman layers interact, allowing for divergence of cross-shelf transport and, consequently, upwelling and downwelling [Lentz, 1995].

Poleward flow is more common on the inner shelf than on the mid and outer shelf, especially near the bottom [Hickey, 1989]. In the cross-shelf direction, current meter observations have shown that the onshore flow compensating for offshore Ekman transport often occurs in the interior region away from the bottom boundary layer, both in mean summer profiles and during individual upwelling events [Smith, 1981; Huyer, 1983; Hickey, 1989].

Mesoscale features are an important source of spatial variation in the along-shelf direction in the northern CCS. Fresh water from the Columbia River influences both the Washington and Oregon shelves during summer [Hickey et al., 2005, 2009], though nutrient concentrations in the plume are typically low compared with upwelled water [Hill and Wheeler, 2002; Bruland et al., 2008]. Juan de Fuca canyon separates the Washington shelf from the British Columbia shelf, and the cyclonic Juan de Fuca eddy appears as a persistent summer feature with ~50 km horizontal scale [Freeland and Denman, 1982; MacFadyen et al., 2005, 2008]. Off Oregon, Heceta Bank deflects the summertime equatorward coastal jet offshore, with increased

retention on the south side of the bank closer to shore [Castelao and Barth, 2005; Barth et al., 2005].

The term “hypoxia” describes low DO conditions, defined here as concentrations < 1.4 mL/L (= 2 mg/L = 62.5 μM ~ 20% saturation for S = 32 and T = 7°C), that can potentially cause physiological stress in marine organisms. In general, the ecosystem impacts of hypoxia vary depending on the typical seasonal cycle of DO, the persistence of hypoxic conditions, and the types of organisms at a specific location [Davis, 1975; Diaz and Rosenberg, 1995]. Diaz and Rosenberg [1995] suggest that, in areas with strong seasonality, mortality begins when DO concentrations fall below 1.0 mL/L and mass mortality occurs at concentrations less than 0.5 mL/L. Fish and crustaceans may be able to avoid hypoxic regions, but are typically less tolerant to low oxygen concentrations than annelids or bivalves, especially during prolonged hypoxic conditions [Gray et al., 2002]. Inner shelf near-bottom water in the northern CCS provides habitat for commercially important species such as Dungeness crabs and English sole [Botsford et al., 1989]. Here, we define “severe hypoxia” as 0.5 mL/L, consistent with Chan et al. [2008].

Depletion of DO in hypoxic environments can be caused by biochemical consumption in the water column and within the bottom sediment. Isolating water column and sediment sinks in a regional numerical model can greatly affect the vertical structure of DO in the water column and the location of hypoxia over the shelf, as shown for the Gulf of Mexico by Hetland and DiMarco [2008]. Surface sediment over the Washington shelf is characterized by a north-northwest oriented silt deposit of Columbia River origin that lies between the 60 and 120 m isobath at the latitude of Grays Harbor, and sandy sediment on the inner shelf which is part of a transgressive layer formed by rising sea levels [McManus, 1972; Nittrouer, 1978]. On the mid to outer shelf, irrigation by benthic infauna enhances fluxes of DO from near-bottom water to sediments [Archer and Devol, 1992; Devol and Christensen, 1993]. Aerobic respiration and oxidation of reduced inorganic species both contribute to sedimentary oxygen demand. Anaerobic forms of respiration, such as denitrification, also occur in the pore waters of shelf sediments. Denitrification consumes nitrate rather than oxygen and does not occur in the water column unless DO concentrations are suboxic, less than 0.1–0.2 mL/L [Codispoti et al., 2005]. On the Washington shelf, aerobic respiration and denitrification both take place in the upper 10 mm of the sediments, primarily in discrete sites surrounding particles of organic matter [Brandes and Devol, 1995]. Fluxes of both DO and nitrate during summer, measured using benthic flux chambers, are always directed into the sediment [Devol and Christensen, 1993; Hartnett and Devol, 2003]. Stoichiometric evidence for denitrification is therefore a potential indicator of sedimentary DO consumption.

In this paper, we first describe the available data sets (Section 2), followed by the historical (1950–1986) spatial and temporal distribution of hypoxia in the bottom water of the northern CCS (Section 3). Next, recent survey data (2003–2006) are used to describe spatial distributions of late summer near-bottom DO and corresponding seasonal wind forcing conditions (Section 4.1). Hydrographic data from this time period are used to evaluate the contribution to the seasonal evolution of hypoxia by a) upwelling; b) variability of DO in source waters; c) biochemical DO consumption; and d) the specific role of sedimentary DO consumption (Section 4.2). Last, the higher frequency response of DO to event scale physical forcing over the inner shelf is examined using time series from moored DO sensors (Section 4.3). In the final section, we relate our results to previous studies in the California Current system and other upwelling systems.

2. Data

2.1. Historical water property data

Historical data for the Washington and Oregon continental shelves from the years 1950–1986 were obtained from archived data at the University of Washington and from the National Oceanographic Data Center's World Ocean Database [Boyer et al., 2006]. Bottom depths in the historical data, if not recorded, were determined by interpolating from the National Geophysical Data Center 3 arc-second US coastal relief model [Divins and Metzger, 2008]. Stations with large discrepancies between recorded bottom depth and the interpolated topography (20 m + 20% of interpolated value) were discarded from the analysis. A summary of hydrographic data collected in the region during this time period is given by Landry et al. [1989]. DO measurements were determined by Winkler titration, accurate to ~0.1% under ideal experimental conditions [Carpenter, 1965a]. However, Carritt and Carpenter [1966] have demonstrated the potential for significant analytical errors through the mid-1960s, ± 1 mL/L at highly saturated concentrations (~5 mL/L) and overestimation by 100% or greater at low concentrations (~0.2 mL/L). No corrections have been made to compensate for analytical errors, but it is possible that hypoxia is underrepresented in the early historical data.

2.2. Recent water property data

During the summers of 2003–2006, temperature (T), salinity (S), and DO data were obtained in the northern CCS as part of two multidisciplinary programs: ECology and Oceanography of Harmful Algal Blooms Pacific Northwest (ECOHAB-PNW) and River Influences on Shelf Ecosystems (RISE) programs (Table 1). Data are available between 46°26′N and 49°08′N for the ECOHAB-PNW cruises, and between 46°15′N and 47°50′N for the RISE cruises. This study primarily uses ECOHAB-PNW data from the Washington shelf between Juan de Fuca Canyon and Grays Harbor (see study area, Fig. 1); RISE data are included for a repeated Grays Harbor transect (GHR, Fig. 1). Maximum cast depths were typically 500 m during ECOHAB-PNW cruises and 200 m during RISE cruises. All hydrographic data from these cruises were collected with a calibrated Sea-Bird Electronics (SBE) 911*plus* conductivity, temperature, and depth (CTD) system. Samples for chlorophyll *a* (Chl *a*) were collected in Niskin bottles attached to the instrumented rosette, and Chl *a* determined using non-acidification in vitro fluorometric analysis [Welschmeyer, 1994] after filtration onto Whatman GF/F filters (0.7 μm nominal pore size). Inorganic nutrient samples were collected in polypropylene tubes from rosette bottles and analyzed using a flow injection Lachat autoanalyzer for nitrate plus nitrite ($NO_3^- + NO_2^-$, hereafter referred to as nitrate or "N") and orthophosphate (PO_4^{3-}, hereafter referred to as phosphate or "P") [Smith and Bogren, 2001;Knepel and Bogren, 2002].

Recent DO data were primarily obtained with profiling SBE 43 sensors. During the September 2006 EH6 cruise, sensor measurements of DO were compared to bottle concentrations determined by Winkler titration [Carpenter, 1965b]. Residuals between the in situ calibration and the factory calibration one year earlier are −0.05, 0.05, 0.12, and 0.35 mL/L at 0, 1, 2, and 5 mL/L, respectively (Fig. 2a). Data from the R/V Wecoma during summer 2005 were corrected using a linear regression of sensor and Winkler titration values presented in Lohan and Bruland [2008]. Factory calibrations from successive cruises on the R/V Wecoma (Seabird Electronics, Bellevue, USA) resulted in small corrections at low concentrations, with residuals of 0.08, 0.21, and 0.68 mL/L for DO values of 1, 2, and 5 mL/L, respectively.

To improve the accuracy of the data from ECOHAB-PNW cruises 1–5, sensors that were not calibrated in situ have been adjusted using stations seaward of the shelf in the historical data set. The mean and standard deviation of DO at temperatures in increments of 0.4°C were calculated for each recent cruise, and for each month in the historical data, at stations with bottom depth >1000 m for data between 42°N and 49°N and east of 126°W. Least-squares

linear regressions of mean DO values, at temperatures where the standard deviation of DO did not exceed 0.25 mL/L in the recent or historical measurements, were then used to correct the sensor data; coefficient of determination values, r^2, were ≥ 0.995 for these relationships during each cruise. To reveal possible biases, the regression obtained from this method was compared with the in situ calibration obtained during the September 2006 EH6 cruise (Fig. 2b). Differences between the two methods were 0.05, 0.02, and 0.09 at DO concentrations of 1, 2, and 5 mL/L, respectively. A different SBE 43 sensor, also calibrated with bottle samples, gave nearly identical results, (historical = 0.965 × calibrated + 0.06 mL/L) during a cruise in July 2007 (not shown or used in the results presented here). Intercepts at 0 mL/L ranged from −0.04 to 0.06 mL/L, consistent with factory and in situ calibrations.

2.3. Moored sensors

Moored sensors were deployed on the Washington shelf as part of the ECOHAB-PNW program during summer and early fall of 2005 and 2006 in water depths ~45 and 35 m (E2, E4, see Fig. 1). At E2, temperature, conductivity and fluorescence were sampled near the surface (4 m). At E4, temperature, conductivity, pressure, fluorescence and DO were sampled 3 m above bottom (32 m). An SBE 16*plus* measured temperature and conductivity; a WETLab ECO-FL measured fluorescence and an SBE 43 measured DO. Fluorescence was converted to units of Chl *a* concentration (μg/l) using factory calibrations. Mooring fluorescence are compared to bottle samples of Chl *a* and/or shipboard fluorescence profiles that have been calibrated with bottle samples when possible ($r^2 = 0.59$, $n = 585$ during EH5; $r^2 = 0.78$, $n = 769$ during EH6). Velocity profiles with 2 m spacing were obtained from an upward looking Teledyne RD Instruments Workhorse Sentinel acoustic Doppler current profiler (ADCP) positioned 9m above bottom (28 m) on the E4 mooring. Unless otherwise stated, all water property and velocity data were low-pass filtered using a cosine-Lanczos filter with a half power point of 46 hr in order to remove tidal and other higher frequency signals. ADCP data were rotated into a coordinate system in which the cross-shelf, x (along-shelf, y), direction has been aligned with the local isobath direction, 20 degrees counterclockwise from true north. The sensitivity of results to this coordinate system rotation will be addressed.

To assess whether biofouling affected moored DO sensors, shipboard DO profiles were obtained within 100 m of the mooring site during 2006. Calibrated shipboard sensor DO concentrations exceeded mooring sensor DO concentrations by 0.15 to 0.31 mL/L in three separate casts at the mooring site over a two week period. The residuals (ship - mooring) are likely attributable to DO gradients in the 1 to 2 m vertical distance separating the two sensors. The largest of these residuals occurred when vertical gradients of 0.3 to 0.5 (mL/L)/m were observed near the bottom (not shown). In 2005, residuals from the nearest stations occupied (located 4.8, 3.6, and 11.4 km from the E4 mooring, respectively) ranged from −0.16 to 0.75 mL/L, with the highest residuals occurring during periods of rapid temporal changes and small residuals −0.1 to 0.1 mL/L occurring over two months after deployment. DO sensors on the moorings did not suffer from serious biofouling; large residuals >0.2 mL/L between mooring and shipboard measurements result from their vertical and horizontal separation.

2.4. Calculation of spatial gradients in DO

Data from CTD surveys and moorings were used to calculate horizontal gradients of DO ($\Delta DO/\Delta y$, $\Delta DO/\Delta x$). Cross-shelf gradients were calculated from pairs of CTD stations. Along-shelf gradients were calculated from near-simultaneous shipboard near-bottom measurements and values from the filtered mooring time series. To remove errors due to vertical gradients between the depths of the shipboard sensor and the mooring sensor, casts with vertical DO gradients greater than 0.1 (mL/L)/m at the bottom of the cast were excluded from the alongshore analysis. However, contamination by cross-shelf variations in DO may still be present. Differences between remaining shipboard measurements and values from the filtered mooring

time series cover a range up to 0.5 mL/L as along-shelf distance approaches zero, with shipboard estimates being higher in most cases (not shown). An error estimate E = (0.5 mL/L)/Δy, where Δy is along-shelf distance, represents the potential bias in calculations of along-shelf gradients and will be shown as error bars on appropriate Figures 11 and 12.

2.5. Wind

Hourly wind speed and direction were obtained from the National Data Buoy Center (NDBC) buoy off Cape Elizabeth, Washington (46041, B41; Fig. 1). These data were rotated into the same coordinate system as the velocity measurements. Alongshore wind stress was computed using the drag coefficient from Large and Pond [1981]. These time series were subsequently low pass filtered and decimated in the same manner as the velocity measurements. As a supplement to direct wind measurements, seasonal wind forcing is described using an upwelling index (1967–2006, www.pfeg.noaa.gov), a measure of offshore Ekman transport computed from gridded atmospheric pressure fields [Bakun, 1973;Schwing et al., 1996]. A cumulative upwelling index (CUI) was obtained by integrating daily upwelling index values over the climatological upwelling season 27 April to 26 September [Schwing et al., 2006]. An alternative method of calculating summer CUI, integrating from the spring minimum of the annual CUI [Pierce et al., 2006], was also utilized.

3. Hypoxia in the historical data record

The historical record of near-bottom DO over the continental shelf covers a broad geographic region (Fig. 1). Because the physical setting varies with cross-shelf location, data were separated into three bottom depth ranges: the inner shelf (0–40 m), midshelf (40–80 m), and outer shelf (80–130 m). The 40 m isobath boundary between the inner shelf and midshelf was chosen based on the principle axis orientation of velocity time series over the Washington shelf in 2005 and 2006 (not shown). An interior region, with no counterclockwise veering of the principle axes with depth, was present at E2 (45 m) but not at E4 (35 m), indicating that the boundary layer interaction is restricted to the region inshore of the 45 m isobath. Over the Oregon shelf we use the same 40 m isobath inner shelf boundary, consistent with the cross-shelf transport calculations of Kirincich et al. [2005]. Historical near-bottom DO data from the inner shelf of Oregon are limited to 59 stations, mostly concentrated on the northern Oregon shelf where the shelf width transitions from broad to narrow, compared with 266 stations over the Washington inner shelf.

The historical data show that low DO in bottom water (10 m from the bottom or less) has occurred in the past over a broad region on northern CCS shelves (Fig. 1), in particular, over much of the Washington shelf. Off the Washington coast, nearly all hypoxic stations occur south of Quinault Canyon. On the southern half of the Washington shelf, from the Copalis Beach line to the Columbia River mouth, hypoxic bottom water has been observed across the entire width of the shelf. Over the northern Oregon shelf, hypoxic bottom water has been observed at several sites on the outer and midshelf, but at only one station on the inner shelf, located near the 40 m isobath at the Columbia River mouth. Further south at the Newport Harbor line, hypoxic stations occur at midshelf and, again, one on the inner shelf. Three hypoxic stations are located south of Newport at the outer and mid shelves. The geographic distribution of hypoxia in the historical data may be strongly influenced by the seasonal distribution of measurements at different latitudes (Fig. 3a). The southern Washington shelf and the Newport Harbor line have better seasonal coverage than other locations. The northern Washington shelf, north of 47°30′N, and the Heceta Bank region, south of 44°30′N, have poor coverage, particularly during July through September. Recent studies have shown that the Heceta Bank region is characterized by weaker circulation and higher Chl *a* than the Newport Harbor line,

and therefore Heceta Bank may be more susceptible to hypoxia [Grantham et al., 2004;Barth et al., 2005].

Hypoxia is observed only during June–September throughout the region (Fig. 3b,c). In the available data, the seasonal minimum of near-bottom DO is lower off Washington than off Oregon over the outer shelf, midshelf and the inner shelf (Fig. 3b,c). Off the Washington coast, minimum DO values at these locations (0.71, 0.49, and 0.62 mL/L) were observed on the outer and midshelf during July, and on the inner shelf during August. Off the Oregon coast, minimum values (0.97, 0.99, and 1.32 mL/L) were observed during September on the outer shelf, and during July on the mid and inner shelves. The differences between minimum summer DO concentrations off Washington and Oregon are greater at the mid and inner shelves than over the outer shelf, and are larger than potential analytical errors at low DO concentrations.

DO concentrations over the inner shelf are more variable than over the mid and outer shelves during summer (Fig. 3b,c). Over the inner shelf of Washington, summer concentrations range from well below hypoxic to the higher concentrations more typical of winter further offshore (Fig. 3b). The Oregon inner shelf shows evidence of this broad range at six stations in August (Fig. 3c). Higher concentrations over the inner shelf during summer, which are not observed at midshelf, are consistent with surface water influencing near-bottom concentrations. A comparison of near-bottom T vs. DO shows that, while these two properties are similar off Washington and Oregon over the midshelf, inner shelf water with DO < 4 mL/L is often warmer off Washington than off Oregon (Fig. 4). It is therefore possible that DO concentrations respond differently to event scale wind forcing at these two locations.

An interannual view of inner shelf data (Fig. 5) shows that hypoxic concentrations have been measured throughout the historical record. Over the Washington inner shelf, hypoxia was measured in all decades where data were collected, except the less frequently sampled 1950s. The higher inner shelf concentrations off Oregon are not a result of sampling different decadal time periods since there are data from both Washington and Oregon in the early–mid 1960s. Taking temporal and spatial sampling limitations into account, historical observations indicate periods of borderline hypoxic concentrations on the inner shelf of Oregon north of Heceta Bank and concentrations well below hypoxic thresholds on the inner shelf of Washington.

4. Processes affecting hypoxia on the Washington shelf: 2003–2006

4.1. Late summer hypoxia and seasonal wind forcing

Hypoxia was present in bottom water over the Washington shelf during September of all four years in the period 2003–2006, under a variety of local seasonal wind forcing conditions (Fig. 6). During these surveys, concentrations below 1 mL/L were measured in all years except 2004, but concentrations below 0.5 mL/L were only observed in 2006. Temporal changes on scales of 5–7 days or less are contained within each map, especially closer to shore. However, as discussed in Section 4.3, “patchiness” in space can also occur. The locations of DO minima in the alongshore and cross shore directions vary between surveys. During September 2003, concentrations below 1 mL/L were observed over the mid to outer shelf, but not over the inner shelf, where concentrations did, however, fall below 1.5 mL/L. During September 2004, DO concentrations below 1.5 mL/L were only observed over the mid to outer shelf, with concentrations increasing toward shore. During September 2005, concentrations below 1 mL/L were observed across the entire shelf inshore of Quinault Canyon, and at the mid to outer shelf farther south. In September–October 2006, concentrations below 0.5 mL/L were present on the mid and inner shelf, but not on the outer shelf. During this cruise, minimum values were close to 0.1 mL/L over the midshelf and close to 0.3 mL/L over the inner shelf. We note that hypoxia has been frequently observed in the bottom water on the southern Vancouver Island shelf, also shown by Freeland and Denman [1982].

Minimum DO concentrations observed over the Washington shelf in September are consistent with the CUI integrated from the spring minimum to the end of the summer (Fig. 6e). The lowest (highest) minimum concentrations were observed following the strongest (weakest) seasonal upwelling favorable winds during 2006 (2004). Intermediate minimum DO concentrations between 0.5 and 1.0 mL/L were observed following CUI closer to average levels during September 2003 and September 2005. The presence of intermediate minimum concentrations during 2005 suggests that the CUI integrated from the spring minimum is a stronger indicator of hypoxia than the CUI integrated from the beginning of the climatological season. However, as discussed in Section 4.2, different combinations of local and remote physical forcing, and biochemical DO consumption, are involved in the seasonal development of hypoxia during these two intermediate years.

Concentrations of DO between 0.5 and 1 mL/L, observed in three of four recent years, have previously been observed in the historical record over the outer, mid and inner shelves of Washington (Fig. 3). In the context of the historical data, only the lowest concentrations measured during September 2006 appear to be unprecedented. The presence of concentrations less than 1 mL/L in September and October also appears to be unusual; these concentrations are more common during July and August in the historical record (Fig. 3).

4.2. Seasonal development of hypoxia in shelf bottom waters

In this section we explore the role of three processes in the seasonal draw down of near-bottom DO concentrations over the Washington shelf: seasonal upwelling circulation, source water variability and respiration. In particular, we differentiate between DO demand in shelf sediments and respiration that occurs in the overlying water column.

a) Upwelling of low DO water over the outer and midshelf—Hydrographic transects across the central Washington shelf during the summer of 2005 capture the seasonal evolution of the intensity and cross-shelf distribution of hypoxia, along with related water properties (Fig. 7). DO contours transitioned from flat to tilted between late May and mid June, similar to isopycnals. The first section was taken six days after a late spring transition was observed off Oregon on 24 May [Kosro et al., 2006]. Isopycnals were level in the middle of the water column over the shelf and slope, with tilting isopycnals only observed near the bottom over the shelf. During June and July, under intermittent local upwelling favorable winds (Fig. 7b), the isopycnals in the mid water column (σ_t = 25–26 kg/m^3) became more tilted over the mid and outer shelf, along with DO contours 4–6 mL/L (Fig. 7a), a likely result of remote forcing by winds further south [Hickey et al., 2006]. In August, upwelling favorable winds intensified (Fig. 7b) and isopycnals outcropped at the surface (Fig. 7a). Through August and September, decreasing DO concentrations at midshelf continued with tilting of mid water column isopycnals; the σ_t = 26.5 kg/m^3 isopycnal approached shore and its height above the bottom increased through 8 September, with slight relaxation apparent between 8 September and 14 September. Thickening DO contours between 2 and 4 mL/L from 8 September to 14 September were associated with decreased stratification, as seen in the spreading of density contours > 26.0 kg/m^3. Throughout the summer, DO contours followed the tilting and vertical separation of isopycnals in the water column.

Minimum DO concentrations over the shelf during 2005 were observed near the bottom, but were not always associated with the densest water (Fig. 7a). On 17 June, 17 July, 23 August, 8 September, and 14 September, minimum near-bottom concentrations were observed inshore of the shelf break. This pattern suggests that respiration draws down DO as water moves shoreward across the shelf from the outer shelf to the midshelf. However, DO concentrations over the mid and outer shelf did not consistently decrease in time through early September as density increases. At the 100 m isobath, near-bottom DO increased from 9 July to 17 July to

5 August, indicating that hypoxia there is either spatially patchy, temporally sporadic, or both. Patterns of DO in near-bottom water are therefore more complex than can be attributed to upwelling of low DO slope water alone.

b) Source water variability—In this section, water properties from the Washington shelf and slope are used to address variability in the composition of water masses in the source water at the shelf break as an additional potential factor in the seasonal development of hypoxia. Stations between the 130 and 1000 m isobaths are defined as "slope" water; stations west of the 1000 m isobath, excluding stations directly within Quinault Canyon, are defined as "offshore" water to represent background properties. For each cruise, the 10–19 offshore casts were averaged into one water property profile (Fig. 8). Discrete samples from standard depths offshore and over the slope, and from near bottom over the outer shelf and midshelf, are included for all stations where nutrient data are available (see Fig. 8f inset). Near-bottom shelf water occurs in T, S and σ_t ranges 7–8°C, 33.4–34.0 psu and 26.1–26.6 kg/m^3, respectively (Figs. 8, 9a).

Offshore water properties vary on seasonal and interannual time scales. Seasonal variability during 2003 and 2005 is associated with changes in T of ~0.5°C or less (Figs. 8a-d, 9b). Larger differences in background properties are associated with interannual variability; low DO in offshore water during September 2006 is associated with a warm anomaly (Figs. 8e,f), up to 1°C warmer than 2003 or 2004 at salinities between 33 and 34 psu (Fig. 9b), consistent with a greater influence of low DO equatorial water [Lynn and Simpson, 1987]. Near-bottom shelf water during this period is also relatively dense (Fig. 8f), suggesting that seasonal upwelling of deep, low DO water is an additional factor in the severe hypoxia during summer 2006. In the range of physical properties occupied by near-bottom shelf water, corresponding offshore DO concentrations are not hypoxic (Figs. 8, 9a). Variability in offshore water masses can therefore only account for seasonal decreases to concentrations as low as ~1.5 mL/L in near-bottom water.

DO concentrations over the slope differ from those offshore, particularly during late summer (Fig. 8), and we next address whether these lower concentrations are associated with a difference in water mass composition over the slope, or biochemical depletion of DO. In the 7.0–8.0°C range, slope DO concentrations reached a minimum of 1.04 mL/L, 1.41 mL/L, 0.83 mL/L, and 0.97 mL/L in 2003, 2004, 2005, and 2006, respectively (Fig. 8). However, there is no evidence of significantly higher T or S over the slope than the offshore averages during 2003, 2004 or 2006 (Figs. 8b,f). During 2005, higher T and S do occur over the slope, resembling the offshore properties earlier that summer in June when slope DO concentrations were higher (Fig. 8d).

These water properties suggest that, in general, hypoxic DO concentrations over the slope result from respiration near the shelf in the northern CCS, not physical transport of equatorial water by the California Undercurrent.

c) Biochemical depletion of DO—Evidence of DO depletion due to biochemical processes is present over the slope and in near-bottom water over the continental shelf during late summer. In particular, relationships between DO, T, and S at these locations do not follow the structure of the offshore properties, especially during late summer (Fig. 8, 9a). In order to quantify the amount of respiration that has influenced each sample over the slope and shelf, we define the DO deficit as the difference between a sample's DO concentration and the average offshore concentration at the same salinity for that cruise. Average offshore relationships between DO and S are not greatly affected by water mass composition, and are similar throughout all six cruises during summers 2003–2006, with $\leq$ 0.5 mL/L difference at constant S (Fig. 9a). In the range of salinity that occurs in shelf bottom water (33.4–34.0 psu), offshore DO concentrations

range from 1.5–4.0 mL/L. This relationship represents the potential contribution to the seasonal draw down of DO by the combination of physical processes already discussed, either seasonal upwelling or an enhanced California Undercurrent, since these processes are both associated with high S and low DO.

Differences in DO deficits between cruises can reveal the contribution to hypoxia not associated with physical processes. For example, there is >0.5 mL/L difference in DO deficit between September 2003 and 2004, even though midshelf bottom water occurs in the same range of salinity (33.4–33.8) for both cruises (Fig. 9a,f). The larger DO deficits in 2003, in a similar range of S, suggest that stronger DO consumption in 2003 is the primary factor causing lower DO concentrations (<1 mL/L) that year.

In contrast, similar DO deficits are observed under varying degrees of hypoxia. For example, DO deficits approached magnitudes of 2.5 mL/L during September 2003, September 2005, and September 2006, although the minimum DO was significantly lower during 2006 (Fig. 9a,f). Bottom water salinity was similar in 2005 and 2006, but high DO concentrations were present in offshore water at these salinity values during 2005 (Fig. 9a). Of these three years, midshelf bottom water salinity was lowest in 2003 (Fig. 9a), consistent with average upwelling favorable winds (Fig. 6e) and a lack of equatorial influence compared with the other years (Fig. 9b). Therefore, physical processes, the enhanced upwelling and the enhanced California Undercurrent described previously, significantly contributed to the extremely low DO concentrations observed in 2006, in addition to biochemical processes.

d) DO consumption in sediments—To distinguish between the water column and sediments as sinks of DO, we use denitrification as an indicator of sedimentary DO consumption, combining measurements from this study and previously published benthic fluxes in order to formulate mass balances of DO and N. We use two separate methods to calculate N deficits, which quantify the amount of N that has been lost to denitrification. Denitrification does not occur in the water column unless DO concentrations fall below ~0.2 mL/L, close to the minimum concentrations observed in September 2006, but not typically associated with hypoxia in the northern CCS. We show that N deficits are correlated with the DO deficits caused by biochemical processes in both the water column and sediments. This relationship, along with benthic fluxes of DO and nutrients from previous studies over the Washington shelf [Devol and Christensen, 1993], are incorporated into a simple mass balance of DO and N in the bottom mixed layer, providing estimates of DO consumption separately in the water column and sediment.

The amount of denitrification that has influenced a water parcel can be quantified by comparing the relationships of observed inorganic nutrient and DO concentrations to those predicted by the stoichiometry of organic matter. The stoichiometry involved in aerobic respiration can be described approximately by the equation [Anderson, 1995]

$$C_{106}H_{175}O_{42}N_{16}P+150\,O_2=106\,CO_2+16\,HNO_3+H_3PO_4+78\,H_2O, \quad (1)$$

which implicitly includes an intermediate step in which ammonium (NH_4^+) is oxidized to nitrate during nitrification in the presence of oxygen. In equation (1), 16 moles of N are produced for every 1 mole of P produced and every 150 moles of DO consumed. Assuming the same chemical composition of organic matter, Gruber and Sarmiento [1997] describe the stoichiometry of denitrification using the equation

$$C_{106}H_{175}O_{42}N_{16}P+104\,NO_3^-=4\,CO_2+102\,HCO_3^-+60\,N_2+36\,H_2O+HPO_4^{2-}, \quad (2)$$

in which 104 moles of N are consumed for every mole of P produced. In Washington shelf sediments, denitrification consumes nitrate that is supplied by fluxes from the overlying water column and nitrate that is produced during nitrification; some portion of ammonium produced during organic matter degradation escapes as a flux out of the sediments [Devol and Christensen, 1993; Hartnett and Devol, 2003]. Deviations from offshore N-P and N-DO ratios in slope water and near-bottom shelf water (Fig. 9c,d) are consistent with the influence of sedimentary denitrification.

Nutrient and DO data from ECOHAB-PNW cruises are used to calculate N deficits, which quantify the amount of N that has been removed from the water by denitrification. The first definition of N deficit, based on N and P concentrations, is similar in form to the N deficit used by Codispoti et al. [2001] in the Arabian Sea and also to the negative of Gruber and Sarmiento's N* [1997] used in their global N budget:

$$\text{N deficit}=\left[\left(r_{aer}^{N:P}\text{P}+c_{aer}^{N:P}\right)-\text{N}\right]*\left(\frac{r_{denitr}^{N:P}}{r_{denitr}^{N:P}-r_{aer}^{N:P}}\right), \quad (3)$$

Where $r_{aer}^{N:P}$ is the stoichiometric ratio of N and P during aerobic respiration as in (1), the constant $c_{aer}^{N:P}$ accounts for limitation of either N or P, and $r_{denitr}^{N:P}$ is the stoichiometric ratio of N and P during denitrification as in (2). We assume $r_{denitr}^{N:P}=104$, following Gruber and Sarmiento [1997], who estimate an uncertainty of ± 15 in this value. We assume that ammonium concentrations are negligible in the calculation of total inorganic nitrogen and its deficit because average ammonium concentrations over the Washington shelf during summer are <1 μM, with maximum values at the inner shelf, away from the stations we are considering in this portion of the analysis [Landry et al., 1989]. Values for $r_{aer}^{N:P}$ and $c_{aer}^{N:P}$, which describe the relationship between N and P away from the influence of denitrification, were determined from a linear regression of offshore N and P data for each ECOHAB-PNW cruise (Fig. 9c). With the exception of the two cruises in 2005 (EH4, EH5), $r_{aer}^{N:P}$ was within the range 14.9–15.7.

To incorporate N deficits into mass balances of N and DO, we have compared N deficits as calculated above with those calculated using an alternate method that uses the N-DO rather than N-P relationships. In the absence of denitrification, Equation (1) suggests that 9.375 moles of DO should be consumed for every mole of N remineralized. Based on this concept, Broecker [1974] developed the tracer

$$\text{NO}=c_{aer}^{DO:N}*\text{N}+\text{DO} \quad (4)$$

where $c_{aer}^{DO:N}$ is the ratio at which DO and N are consumed and remineralized during aerobic respiration. N deficit can be expressed as

$$\text{N deficit}=\frac{[\text{NO}_{expected}-\text{NO}]}{c_{aer}^{DO:N}} \quad (5)$$

where $NO_{expected}$ is the value of NO away from the influence of denitrification. We utilize the average offshore NO in the salinity range 32.8 < S < 34.0 for each cruise, which results in values of $NO_{expected}$ = 425 ± 14 μM. Our two methods of calculating N deficit agree, except for the two cruises in 2005 where offshore relationships between DO, N, and P appear to be anomalous (Fig. 9c,d,e). We utilize the NO method in the following analysis and test the sensitivity of our results to the anomalous 2005 data.

N deficits and DO deficits in near-bottom water and 100–200m slope water for all six ECOHAB-PNW cruises are linearly related (Fig. 9f). The linear regression ($r^2 = 0.77$, $p < 0.01$) was calculated using a geometric mean functional technique [Ricker, 1984]. The slope of the regression decreases slightly from 11.1 to 10.9 when anomalous 2005 data are removed. While there is some evidence of N and DO deficits in slope water, their largest values are ~1/2 as high as those over the mid to outer shelf (Fig. 9f).

Simplified mass balances of N and DO can be used to calculate the relative importance of respiration in the water column and sediments. In a bottom mixed layer overlying the sediment, biochemical changes in N and DO can be expressed as

$$\frac{dN}{dt} = \frac{1}{h_{BML}}\left(f_{sed}^{NO_3^-} + f_{sed}^{NO_2^-} + f_{sed}^{NH_4^+}\right) - \frac{1}{c_{aer}^{DO:N}} k_{wc}^{DO} \tag{6a}$$

$$\frac{dDO}{dt} = \frac{1}{h_{BML}}\left(f_{sed}^{DO} - \frac{1}{2} f_{sed}^{NO_2^-} - 2 f_{sed}^{NH_4^+}\right) + k_{wc}^{DO} \tag{6b}$$

where d/dt is the material derivative following a parcel of near-bottom water, f_{sed} represents a flux from the sediment into the water column, h_{BML} is the bottom mixed layer height, and k_{wc}^{DO} is the water column rate of aerobic respiration. These equations assume that all nitrite and ammonium that escape the sediment are oxidized to nitrate. Utilizing the chain rule and applying Equations 4 and 5,

$$\frac{d(DO\ \text{deficit})}{d(N\ \text{deficit})} = \frac{dDO}{dt} \Big/ \left(\frac{1}{c_{aer}^{DO:N}} \frac{dDO}{dt} + \frac{dN}{dt}\right), \tag{7}$$

gives an expression for the water column rate,

$$k_{wc}^{DO} = \left[k_{sed}^{N} \frac{d(DO\ \text{deficit})}{d(N\ \text{deficit})} + k_{sed}^{DO}\left(\frac{1}{c_{aer}^{DO:N}} \frac{d(DO\ \text{deficit})}{d(N\ \text{deficit})} - 1\right)\right], \tag{8}$$

where k_{sed}^{N} and k_{sed}^{DO} are the rates of change of N and DO in the bottom mixed layer due to sediment fluxes, including those associated with oxidation of nitrite and ammonium. Means and 95% confidence intervals for all parameters used to estimate k_{wc}^{DO} are shown in Table 2. The bottom mixed layer height h_{BML} is estimated as the height over the bottom at which vertical DO gradients exceed 0.1 (mL/L)/m (a temperature gradient criterion of 0.01 °C/m gives similar results). The relationship $d(DO\ \text{deficit})/(d\ N\ \text{deficit})$ is given by the slope of the regression in Fig. 9f. Sediment fluxes from previous studies were measured using benthic tripods over the

Washington shelf and slope during June and July of 1989 and 1991 [Devol and Christensen, 1993]. Published flux values used for this analysis are from bottom depths < 200 m to capture only processes occurring on the continental shelf and upper slope. The shallowest benthic flux measurement was at 42 m bottom depth off Grays Harbor, and bottom water DO concentrations were 1.5–2.5 mL/L [Devol and Christensen, 1993]. The standard error (2σ) of the mass balance results are calculated using a Monte Carlo method (10^6 runs), with parameters having Student t-distributions as described in Table 2.

The mass balances of DO and N can indicate whether the observed relationship between DO and N deficits are consistent with a significant contribution to aerobic respiration from the sediment. The calculated water column rate, k_{wc}^{DO}, is −0.021 ± 0.007 (mL/L)/d, or 0.92 ± 0.30 μM/d; the sedimentary DO flux into the bottom mixed layer results in a similar rate, −0.020 ± 0.005 (mL/L)/d, or −0.90 ± 0.21 μM/d; and oxidation of the ammonium flux from the sediments contributes a small amount, −0.002 (mL/L)/d; or 0.09 μM/d. The mass balance also results in a small N increase, 0.032 ± 0.020 μM/d, which suggests that the combination of the ammonium flux from the sediments and the mineralization of N during water column respiration balances the loss of near-bottom N to denitrification in sediments.

Results from the mass balance indicate that DO consumption in the water column and sediments contribute similarly, 40–60% each, to the rate of decrease of DO in near-bottom water. Further support for these estimates of DO consumption is obtained from time series of DO from moored sensors. The data display a significant downward trend over several weeks during both 2005 and 2006 (Fig. 10a). Since this trend is not coincident with decreasing temperatures (Fig. 10b), declining DO at this location is likely due to respiration, not upwelling of progressively colder water from further offshore. The total DO consumption calculated from the mass balance agrees well with the observed downward trends in both years. The DO decline during 2006 follows a bloom in the surface layer (Fig. 10c), which occurred before the start of the DO time series. A period of relatively high surface fluorescence, confirmed by Chl *a* concentrations 6.5–17.0 μg/L in bottle samples, continued through the DO time series (Fig. 10c). During 2005, satellite data indicate a transition from negative to positive Chl *a* anomalies during July [Thomas and Brickley, 2006], which precedes the start of the DO decline in early August (Fig. 10a).

4.3. Event time scale variability in DO of shelf bottom water

In addition to seasonal trends, DO time series from moored sensors exhibit significantly shorter period fluctuations (Fig. 10a). During late August–September 2005, four events with amplitude 0.6–1.0 mL/L are observed, each lasting 5 to 10 days. During 2006, there are fewer events of this magnitude and duration. There are, however, two relatively sharp decreases of DO over the course of the 2006 time series starting 11 September and 28 September, as well as a peak above 5 mL/L. This section will explore the short time scale processes that result in these DO fluctuations. The rate of change in DO concentration due to horizontal advection is given by the equation

$$\frac{\partial O}{\partial t} = -u\frac{\partial O}{\partial x} - v\frac{\partial O}{\partial y}, \tag{9}$$

where $\partial O/\partial t$ is the time rate of change of DO; u, v are the cross-shelf and along-shelf components of the velocity; and $\partial O/\partial x$, $\partial O/\partial y$ are the cross-shelf and along-shelf components of the spatial gradient of DO. In the following, we use hydrographic data and moored sensor data to provide estimates of the individual contributions from these two components to DO variability over time scales of several days.

During mid August through late September 2005, upwelling favorable winds were frequently interrupted by relaxation and weak downwelling events, in contrast to the persistent upwelling that characterized the preceding period from mid July through mid August (Fig. 6e). From 24 August to 14 September, the phase relationship between $\partial O/\partial t$ and v is out of phase; increasing (decreasing) DO concentrations coincided with equatorward (poleward) flow (Fig. 11a). After 14 September, the phase relationship between $\partial O/\partial t$ and v shifted to be in phase; increasing (decreasing) DO concentrations coincided with poleward (equatorward) flow. Overall, the time series are consistent with alongshore advection of a low DO patch that begins south of the mooring, then moves north of the mooring during a period of prolonged poleward flow and relatively weak winds (Fig. 11a,b).

This period of alternating upwelling and downwelling conditions over the inner shelf was accompanied by the appearance of higher near-bottom fluorescence at E4 (Fig. 11c). Calibrated shipboard fluorescence data from nearby stations E2 and two nearby stations on the Kalaloch Beach (KB) line are consistent with the moored sensor (Fig. 11c); no casts were taken exactly at the mooring site. Although peaks in near-bottom fluorescence are small compared to values typically observed with a bloom in the euphotic zone, the presence of photosynthetic pigment near the bottom suggests that organic matter, and the potential for respiration, has been introduced to the bottom water, either by sinking, advection, or resuspension of particles.

To further assess whether the advection of an alongshore patch can account for the magnitude and timing of DO fluctuations during this period in 2005, we have estimated time integrals of the advective terms on the right hand side of (9), for direct comparison with the DO time series. In the cross-shelf calculation, gradients are taken from the KB line, the transect closest to the mooring, and the integral evaluated forwards and backwards in time until the integrated cross-shelf velocity exceeds the distance to KB stations on the shelf. Gradients at the KB line are small during this period; we also use the largest gradient shown in Fig. 11d in order to generate larger cross-shelf fluctuations and compare their timing to observations. In the along-shelf direction, both positive and negative gradients occur, supporting the idea of an along-shelf minimum in DO (Fig. 11d). The largest observed gradient is applied, positive poleward of the patch center and negative equatorward of a patch center. This choice ensures that gradients are not underestimated during periods when the hypothesized patch is between the mooring and ship. The integration is started on 22 August, soon after the appearance of near-bottom fluorescence (Fig. 11c).

In the cross-shelf direction, the modeled fluctuations show no significant correlation with the observed data, and the magnitude of the fluctuations are far too small, even with the relatively large non-local gradient (Fig. 11e). Because the cross-shelf velocity is sensitive to the direction in which the coordinate system is rotated, results using a coordinate system rotated 10 degrees in either direction are also shown (Fig. 11e), with little improvement of the results. The along-shelf integration is far more successful in reproducing the observed time series (Fig. 11f). In this case, modeled fluctuations have the correct timing to account for the observations. Additional results are shown with a constant trend, the total respiration calculated in Section 4.2 d (Fig. 10a), to account for large scale respiration over the shelf, and also with a reduction of velocity by 50% to account for the effects of bottom friction in reducing the velocity between the current meter and the DO sensor. Though a strictly linear interpolation with a no-slip condition would result in a 75% reduction in velocity, a realistic velocity profile has more of a logarithmic shape; at E2, the difference between v at 13 m and 7 m above the bottom is never more than 10% during this time period (not shown). While the simple trend improves agreement with the data, the velocity reduction results in a slight underestimate of the magnitude of the fluctuations (Fig. 11f). In addition, the observed DO increase starting on 14 September occurs too late in the model, which predicts an increase when the patch passes by the mooring site on

18 September. This inconsistency may be a consequence of downward vertical advection during prolonged poleward flow on the inner shelf (Fig. 11a).

Fluctuations in DO concentration during 2006 are typically much weaker than in 2005, with the exception of one high DO event (Fig. 10). During this event, DO concentrations increase beginning 15 September, along with acceleration to poleward flow which later peaks in excess of 20 cm/s (Fig. 12a). DO concentrations return to hypoxic levels beginning 23 September, within days after upwelling winds resume (Fig. 12b). On this date, flow 12 m above the bottom is poleward and offshore, which is inconsistent with upwelling. However, since temperature also dropped by >2 °C (Fig. 10b), the decrease in DO is likely due to unresolved onshore transport in the bottom boundary layer, not biochemical consumption.

Two additional notable decreases in DO during 2006, ~0.4–0.6 (mL/L)/d, occur on 11 September and 28 September (Fig 12a). These events occur during strong upwelling favorable winds (Fig. 12b) and also follow peaks in near-bottom fluorescence (Fig. 12c), although the magnitude of the fluorescence peaks is not as great as in 2005 (Fig. 11c). Shipboard measurements at the mooring site confirm low background fluorescence levels (Fig. 12c); Chl *a* concentrations from bottle samples exceed the mooring values by 1–2 μg/L, and the shipboard fluorometer agrees more closely with the mooring. Cross-shelf transport was integrated in a similar manner as the 2005 analysis, using spatially variable gradients from the KB line near the mooring. These KB transects have strong positive gradients at the two stations closest to shore (Fig. 12d), and weak negative DO gradients further offshore corresponding to midshelf minima (Fig. 6d, e.g.). The cross-shelf models reproduce the decreases in DO beginning 11 September and 28 September, and the gradual increase in DO beginning 30 September (Fig. 12e). The models fail to predict the onset of the large peak in DO, and the timing of the return to hypoxia following the peak.

Along-shelf advection does not appear to be as important during 2006 as 2005. The only strong along-shelf gradients are positive and appear during the onset of the strong poleward wind event after 15 September; those measured closest in time to the decreasing DO events are smaller, between 0.0–0.015 (mL/L)/km, at the same time when large cross-shelf gradients are observed (Fig. 12d). An alongshore integration with a gradient of (0.05 mL/L)/km increasing northward results in increasing DO concentrations during the three periods where observations show significant decreases (Fig. 12f). Using a smaller alongshore gradient of 0.015 mL/L, with a 50% velocity reduction and trend as in the 2005 analysis, eliminates event scale variability and more accurately reproduces longer term variability (Fig. 12f). The lack of alongshore variation in DO during 2006, in contrast to 2005, suggests that the bloom observed in the surface layer (Fig. 10c) resulted in DO consumption over a greater along-shelf scale during 2006. A large region of low DO in the near-bottom water along the midshelf, consistent with the 2006 survey map (Fig. 6d), allowed for rapid return to severe hypoxia over the inner shelf within several days, even after strong downwelling favorable winds.

5. Discussion and summary

In this paper, historical and recent hydrographic data, as well as moored sensors, are used to investigate spatial patterns of hypoxia in the northern CCS and its temporal variability from days to decades. We show that, off Washington 1) hypoxia occurs under a wide range of wind forcing conditions and source water properties; 2) biochemical DO consumption in both the water column and sediments is a significant factor in the development of hypoxia; 3) advection of patches with spatial scales ~10–50 km can lead to short term variability; and 4) in contrast to historical measurements over the Oregon shelf, DO concentrations below 1 mL/L are a recurring feature in the historical record, including the inner shelf.

The results of this study emphasize the fact that hypoxia is a seasonal feature of the northern CCS. Hypoxia is present in near-bottom water throughout the historical record (Fig. 4), and was observed off the Washington shelf during all four recent September surveys (Fig. 6). The strength of the seasonal upwelling favorable winds appears to be an important factor in the severity of hypoxia at the mid-outer shelf, with stronger upwelling favorable winds associated with lower minimum DO concentrations over the Washington shelf, as seen most dramatically during 2006.

Over the Washington shelf, interannual differences in near-bottom DO are related in part to the biological response to upwelling. Not only do upwelling events increase phytoplankton standing stock in the euphotic zone by supplying nutrients, persistent upwelling may also promote near-bottom respiration by retaining sinking material closer to the shelf [Hales et al., 2006]. Furthermore, hypoxic bottom waters promote increased concentrations of iron (II) in near-bottom water, which could enhance primary production if that water is upwelled to the euphotic zone [Lohan and Bruland, 2008]. Our results from recent data demonstrate that cross-shelf transport of offshore water and interannual changes in its water mass composition can only account for decreases to concentrations as low as ~1.5 mL/L; shelf DO concentrations at salinity between 33.4 and 34.0 psu indicate that biochemical consumption typically decreases concentrations by an additional 0.5–2.5 mL/L, depending on the year and location (Fig. 10a). Weak upwelling favorable winds during late August and September 2004 (Fig. 6) likely kept DO deficits, which indicate biochemical depletion of DO, relatively low by limiting primary productivity and subsequent respiration. Although much of the September 2004 data were collected during a period of strong downwelling favorable winds [MacFadyen et al., 2008], such events primarily replenish DO on the inner shelf (Section 4.3, Fig. 12).

During summer 2006, several factors coincided to allow severe hypoxia to occur over the Washington shelf. Compared with September 2003, near-bottom shelf water during September 2006 had similar DO deficits but higher salinity (Fig. 9a), consistent with lower DO source water due to enhanced seasonal upwelling favorable winds (Fig. 6) and a strong California Undercurrent as indicated by a warm anomaly (Fig. 9c,d). It may be surprising that DO deficits do not indicate a stronger biological response in September 2006 following strong seasonal upwelling favorable winds. However, it is possible that stronger DO deficits in September 2006 were not observed only because low DO concentrations inhibited additional respiration in the water column and/or sediments. Compared with 2005, which was characterized by strong upwelling during the later part of the season only, near-bottom shelf water during 2006 was characterized by similar decreasing DO trends in mooring time series (Fig. 10), but less “patchiness”. Water column respiration may have been responsible for the observed patchiness during 2005, since a stationary patch of enhanced sediment respiration is less likely to form a well defined patch in the overlying moving water column. Strong upwelling winds throughout the entire summer of 2006, instead of just the late season, may have created conditions where fresh organic matter was readily available to be processed by respiration over the entire shelf, instead of in isolated locations.

The presence of N-P and N-DO relationships in near-bottom water that have been influenced by denitrification in sediment pore water (Fig. 9c–f) indicate that DO consumption in shelf sediments is an important biochemical contribution to the development of seasonal hypoxia, in addition to respiration in the water column. Simple mass balances of DO and N relate recently collected water column data to previously published fluxes at the Washington shelf during early summer [Devol and Christensen, 1993]. There do not appear to be seasonal changes in the relationship between near-bottom DO deficits and N deficits from early to late summer during 2003 and 2005 (Fig. 9f), but it is possible high N deficits observed during September 2006 are associated with changes in sediment processes during severely hypoxic conditions. As DO concentrations decrease, fluxes of DO into the sediments should theoretically decrease

due to reduced pore water irrigation by benthic macrofauna [Archer and Devol, 1992], and fluxes of nitrate should increase [Middelburg et al., 1996].

Our estimated average water column respiration rate, 0.021 (mL/L)/d (or 0.92 μM/d), is consistent with measurements of water column respiration in coastal upwelling regions of the Eastern Atlantic, which indicate that respiration rates below 1 μM/d can occur at water depths >50 m even below productive surface waters [Robinson et al., 2002]. Higher respiration rates, ~3 μM/d, were measured in this depth range off the coast of Namibia in association with high bacterial abundances [Robinson et al., 2002], and it is possible that water column respiration rates vary within the northern CCS. Depletion of DO over the Washington shelf is slow compared with the Gulf of Mexico hypoxic zone, where near-bottom DO can decline at a rate of ~0.15–0.20 (mL/L)/d (or 6.7–8.9 μM/d) [Rabalais et al., 2007]. The more rapid depletion in the Gulf of Mexico is associated with higher sedimentary DO consumption [Rowe and Chapman, 2002] and water column respiration rates [Dortch et al., 1994]. Respiration in near-bottom water over the Washington shelf balances ~7–13% of the primary productivity (~1–2 g C m^{-2} d^{-1} [Perry et al., 1989]).

Over the inner shelf of Washington, DO concentrations do not always respond to wind as expected by simple two dimensional dynamics, particularly when respiration results in significant along-shelf gradients. During 2005, low DO concentrations on the inner shelf appeared during both upwelling and downwelling favorable winds, and were controlled by the alongshore advection of an isolated patch of low DO rather than by cross-shelf transport (Fig. 11e,f). It is possible that patchiness may be more prevalent off Washington than Oregon. Since inner shelf hypoxia is present under a broader range of temperatures in the historical measurements off Washington than Oregon (Fig. 4), patches of low DO may be able to persist under a wider range of short term wind forcing rather than just the strongest upwelling events and therefore may account for a greater portion of the event scale variability.

The lower DO concentrations off Washington compared with Oregon in the historical record (Figs. 3, 4) are likely related to differences in physical and biological dynamics. Ware and Thomson [2005] and Hickey and Banas [2008] show that the coast of Washington and the southern coast of British Columbia are the most highly productive regions along the western coast of North America. Greater shelf width, nutrients from the Juan de Fuca eddy, mixing in estuaries, enhanced upwelling over submarine canyons, coastal trapped waves, and differential impacts of grazing may play a role in maintaining higher primary productivity despite stronger upwelling winds to the south [MacFadyen et al., 2008;Hickey and Banas, 2008;Banas et al., 2009]. Recent observations show that microzooplankton consume an average of 66% of primary production during summer in the northern CCS, and are therefore a strong regulator in the fate of organic matter [Lessard and Frame, 2008]. Thus, the physical and biological dynamics which lead to hypoxia off the coast of Washington, while linked to processes occurring over the broader California Current region, are also uniquely determined by the specific setting.

Despite the seasonal presence of hypoxia, and extremely low DO concentrations in 2006, the Washington shelf is not typically anoxic like many other upwelling systems. Anoxic conditions elsewhere have arisen from several sets of unique conditions, and demonstrate the sensitivity of hypoxia in upwelling systems to changes in local productivity and large scale physical forcing. Anoxia on the Peru shelf is less prevalent during El Niño years, which are associated with warm anomalies and decreased primary productivity [Barber and Chavez, 1983; Arntz et al., 1991]. Anoxia in Peru also appears to be sensitive to declines in planktivorous fish populations because reduction in grazing allows more organic material to accumulate and degrade [Walsh, 1981]. On the Namibian shelf off southwest Africa, upwelling occurs year round, but anoxia is generated alongside a seasonal shift in the proportion of high DO (> 4 mL/

L) and hypoxic (< 1 mL/L) source waters [Monteiro et al., 2006]. In this case, equatorward flow associated with stronger upwelling can actually inhibit the formation of anoxia by increasing the proportion of high DO and low nutrient source water, and also by decreasing the residence time over which respiration acts [Brüchert et al., 2006]. Over the western Indian shelf, upwelling of nutrients forced by remote winds occurs simultaneously with reduced ventilation and anthropogenic nutrient loading from monsoon river runoff, leading to seasonally anoxic conditions [Naqvi et al., 2006]. Off the Washington coast, advection and respiration create a situation where summer DO concentrations are typically hypoxic, rather than anoxic, supporting a benthic ecosystem that ranks between the severely hypoxic Peru shelf and the relatively high DO northwest Africa shelf in abundance of benthic macrofauna [Jumars and Banse, 1989].

An important question is whether hypoxic events are becoming more severe in the northern California Current system. It has been hypothesized that an increase in upwelling favorable wind stress, in response to warming temperatures, could push upwelling systems past a tipping point where anoxia becomes prevalent [Bakun and Weeks, 2004]. The specific mechanism proposed by Bakun and Weeks [2004] is that intense and persistent upwelling favorable winds would push zooplankton out of the shelf region before they are able to consume faster-growing phytoplankton, which, in the absence of planktivorous fish, would cause more organic matter to reach the shelf sediments. Although intensified equatorward winds do not appear to be strongly influencing the northern CCS when compared with the central and southern California coasts to the south [Schwing and Mendelssohn, 1997], the presence of an intrusion of nutrient rich subarctic water during a hypoxic event off Oregon in 2002 [Grantham et al., 2004], not present in 2006, shows that there are several different potential mechanisms leading to severe hypoxia. Bograd et al. [2008] have observed significant declines of DO between the years 1984 and 2006 in the CalCOFI region, including California Undercurrent water. With high productivity, and a history of seasonal hypoxia, the northern CCS may be particularly sensitive to a comparable decline of DO in this same water.

Acknowledgments

We are grateful to Jim Postel (UW) who originally compiled the historical data set, Nancy Kachel (UW) who was responsible for cruise logistics and processing hydrographic data, Katherine Krogslund's UW lab who assisted with DO samples and Julian Herndon (RTC/SFSU) who performed and processed all the nutrient analyses. A special thanks is extended to the entire sea-going ECOHAB-PNW and RISE teams who were responsible for the massive data collection efforts on multiple cruises. Piers Chapman and two anonymous reviewers provided helpful comments during the revision phase. This work was supported by the PNW Center for Human Health and Ocean Sciences (National Institutes of Health (NIH)/National Institute of Environmental Health (NIEHS): P50 ES012762 and National Science Foundation (NSF): OCE 0434087), by the Coastal Ocean Program of the National Oceanic and Atmospheric Administration (NOAA) (NA17OP2789) and NSF (OCE 0234587) as part of the ECOHAB-PNW project. Additional support was provided by NOAA (NA17RJ1232) as part of the GLOBEC Northeast Pacific program. RISE data were collected with support from NSF (OCE 0239089). Mooring data were collected under National Marine Sanctuary Permits OCNMS-2003-002 and OCNMS-2006-004. This is GLOBEC contribution 665, ECOHAB contribution 299, ECOHAB-PNW contribution 22, and RISE contribution 46. The contents are solely the responsibility of the authors and do not necessarily represent the official views of the NIEHS, NIH, NOAA, or NSF.

Reference List

Anderson LA. On the hydrogen and oxygen content of marine phytoplankton. Deep Sea Res 1995;42(9): 1675–1680.

Archer D, Devol A. Benthic oxygen fluxes on the Washington shelf and slope: A comparison of in situ microelectrode and chamber flux measurements. Limnol Oceanogr 1992;37:614–629.

Arntz, WE.; Tarazona, J.; Gallardo, VA.; Flores, LA.; Salzwedel, HS. Benthos communities in oxygen deficient shelf and upper slope areas of the Peruvian and Chilean Pacific coast, and changes caused by El Niño. In: Tyson, RV.; Pearson, TH., editors. Modern and Ancient Continental Shelf Anoxia. The Geological Society; London, U.K: 1991. p. 131-154.

Bakun, A. NOAA Tech Rep NMFS SSRF-671. US Department of Commerce; Washington D. C: 1973. Coastal upwelling indices, West Coast of North America, 1946–71; p. 114

Bakun A, Weeks SA. Greenhouse gas buildup, sardines, submarine eruptions and the possibility of abrupt degradation of intense marine upwelling ecosystems. Eco Letts 2004;7:1015–1023.

Banas NS, Lessard EJ, Kudela RM, MacCready P, Peterson TD, Hickey BM, Frame E. Planktonic growth and grazing in the Columbia River plume region: A biophysical model study. J Geophys Res 2009;114:C00B06.10.1029/2008JC004993

Barber RT, Chavez FP. Biological consequences of El Niño. Science 1983;222:1203–1210. [PubMed: 17806711]

Barth JA, Pierce SD, Castelao RM. Time-dependent, wind-driven flow over a shallow midshelf submarine bank. J Geophys Res 2005;110:C10S05.10.1029/2004JC002761

Bograd SJ, Castro CG, Di Lorenzo E, Palacios DM, Bailey H, Gilly W, Chavez FP. Oxygen declines and the shoaling of the hypoxic boundary in the California Current. Geophys Res Letts 2008;35:L12607.10.1029/2008GL034185

Botsford, LW.; Armstrong, DA.; Shenker, JM. Oceanographic influences on the dynamics of commercially fished populations. In: Landry, MR.; Hickey, BM., editors. Coastal Oceanography of Washington and Oregon. Elsevier; Amsterdam, The Netherlands: 1989. p. 511-565.

Boyer, TP.; Antonov, JI.; Garcia, HE.; Johnson, DR.; Locarnini, RA.; Mishonov, AV.; Pitcher, MT.; Baranova, OK.; Smolyar, IV. Introduction, NOAA Atlas NESDIS. Vol. 1. Vol. 60. NOAA; Silver Spring, Md: 2006. World Ocean Database 2005.

Brandes JA, Devol AH. Simultaneous nitrate and oxygen respiration in coastal sediments: Evidence for discrete diagenesis. J Mar Res 1995;53:771–797.

Broecker W. “NO” a conservative water-mass tracer. Earth Planet Sci Lett 1974;23:100–107.

Brüchert, V.; Currie, B.; Peard, KR.; Lass, U.; Endler, R.; Dübecke, A.; Julies, E.; Leipe, T.; Zitzmann, S. Biogeochemical and physical control on shelf anoxia and water column hydrogen sulphide in the Benguela coastal upwelling system off Namibia. In: Neretin, LN., editor. Past and Present Water Column Anoxia. Springer; Dordrecht, The Netherlands: 2006. p. 161-193.

Bruland KW, Lohan MC, Aguilar-Islas AM, Smith GJ, Sohst B, Baptista A. Factors influencing the chemistry of the near-field Columbia River plume: Nitrate, silicic acid, dissolved Fe, and dissolved Mn. J Geophys Res 2008;113:C00B02.10.1029/2007JC004702

Carpenter JH. The accuracy of the Winkler method for dissolved oxygen. Limnol Oceanogr 1965a; 10:135–140.

Carpenter JH. The Chesapeake Bay Institute technique for the Winkler dissolved oxygen method. Limnol Oceanogr 1965b;10:141–143.

Carritt DE, Carpenter JH. Comparison and evaluation of currently employed modifications of the Winkler method for determining dissolved oxygen in seawater; a NASCO report. J Mar Res 1966;24:286–318.

Castelao RM, Barth JA. Coastal ocean response to summer upwelling favorable winds in a region of alongshore bottom topography variations off Oregon. J Geophys Res 2005;110:C10S04.10.1029/2004JC002409

Chan F, Barth JA, Lubchenco J, Kirincich A, Weeks H, Peterson WT, Menge BA. Emergence of anoxia in the California Current large marine ecosystem. Science 2008;319:920. [PubMed: 18276882]

Codispoti LA, Brandes JA, Christensen JP, Devol AH, Naqvi SWA, Paerl HW, Yoshinari T. The oceanic fixed nitrogen and nitrous oxide budgets: Moving targets as we enter the anthropocene? Scientia Marina 2001;65(Supl 2):85–105.

Codispoti, LA.; Yoshinari, T.; Devol, AH. Suboxic respiration in the oceanic water column. In: del Giorgio, PA.; le Williams, PJB., editors. Respiration in Aquatic Ecosystems. Oxford University Press; New York: 2005. p. 225-247.

Davis JC. Minimal dissolved oxygen requirements of aquatic life with emphasis on Canadian species: a review. J Fish Res Board Can 1975;32:2295–2332.

Devol AH, Christensen JP. Benthic fluxes and nitrogen cycling in sediments of the continental margin of the eastern North Pacific. J Mar Res 1993;51:345–372.

Diaz RJ, Rosenberg J. Marine benthic hypoxia: a review of its ecological effects and the behavioural responses of benthic macrofauna. Oceanogr Mar Bio Annu Rev 1995;33:245–303.

Divins, DL.; Metzger, D. NGDC Coastal Relief Model. Natl. Geophys. Data Cent; Boulder, Colo: 2008. retrieved 28 April 2008, http://www.ngdc.noaa.gov/mgg/coastal/coastal.html

Dortch Q, Rabalais NN, Turner RE, Rowe GT. Respiration rates and hypoxia on the Louisiana shelf. Estuaries 1994;17:862–872.

Freeland HJ, Denman KL. A topographically controlled upwelling centre off southern Vancouver Island. J Mar Res 1982;40(4):1069–1093.

Grantham BA, Chan F, Nielsen KJ, Fox D, Barth JA, Huyer A, Lubchenco J, Menge BA. Upwelling-driven nearshore hypoxia signals ecosystem and oceanographic changes in the northeast Pacific. Nature 2004;429:749–754. [PubMed: 15201908]

Gray JS, Wu RS, Or YY. Effects of hypoxia and organic enrichment on the marine environment. Mar Ecol Prog Ser 2002;238:249–279.

Gruber N, Sarmiento JL. Global patterns of marine nitrogen fixation and denitrification. Global Biogeochem Cycles 1997;11:235–266.

Hales B, Karp-Boss L, Perlin A, Wheeler PA. Oxygen production and carbon sequestration in an upwelling coastal margin. Global Biogeochem Cycles 2006;20:GB3001.10.1029/2005GB002517

Hartnett HE, Devol AH. Role of a strong oxygen-deficient zone in the preservation and degradation of organic matter: A carbon budget for the continental margins of northwest Mexico and Washington State. Geochim Cosmochim Acta 2003;67(2):247–264.

Hetland RD, DiMarco SF. How does the character of oxygen demand control the structure of hypoxia on the Texas–Louisiana continental shelf? J Mar Syst 2008;10:49–62.

Hickey BM. The California current system—hypotheses and facts. J Phys Oceanogr 1979;8:191–279.

Hickey, BM. Patterns and processes of circulation over the Washington continental shelf and slope. In: Landry, MR.; Hickey, BM., editors. Coastal Oceanography of Washington and Oregon. Elsevier; Amsterdam, The Netherlands: 1989. p. 41-115.

Hickey, BM. Coastal oceanography of western North America from the tip of Baja California to Vancouver Island. In: Robinson, AR.; Brink, KH., editors. The Sea. John Wiley & Sons, Inc; New York: 1998. p. 345-393.

Hickey BM, Banas NS. Why is the Northern End of the California Current System So Productive? Oceanography 2008;21(4):90–107.

Hickey B, Geier S, Kachel N, MacFadyen A. A bi-directional river plume: The Columbia in summer. Cont Shelf Res 2005;25:1631–1656.

Hickey B, MacFadyen A, Cochlan W, Kudela R, Bruland K, Trick C. Evolution of chemical, biological, and physical water properties in the northern California Current in 2005: Remote or local wind forcing? Geophys Res Letts 2006;33:L22S02.10.1029/2006GL026782

Hickey B, McCabe R, Geier S, Dever E, Kachel N. Three interacting freshwater plumes in the northern California Current System. J Geophys Res 2009;114:C00B03.10.1029/2008JC004907

Hill JK, Wheeler PA. Organic carbon and nitrogen in the northern California current system: comparison of offshore, river plume, and coastally upwelled waters. Prog Oceanogr 2002;53:369–387.

Huyer A. Coastal upwelling in the California current system. Prog Oceanogr 1983;12:259–284.

Jumars, PA.; Banse, K. Benthos and its interaction with bottom boundary layer processes. In: Landry, MR.; Hickey, BM., editors. Coastal Oceanography of Washington and Oregon. Elsevier; Amsterdam, The Netherlands: 1989. p. 349-365.

Kirincich AR, Barth JA, Grantham BA, Menge BA, Lubchenco J. Wind-driven inner-shelf circulation off central Oregon during summer. J Geophys Res 2005;110:C10S03.10.1029/2004JC002611

Knepel, K.; Bogren, K. Tech Rep. Lachat Instruments; Milwaukee, WI: 2002. Determination of orthophosphate by flow injection analysis: QuikChemR Method 31-115-01-1-H; p. 14

Kosro PM, Peterson WT, Hickey BM, Shearman RK, Pierce SD. Physical versus biological spring transition: 2005. Geophys Res Letts 2006;33:L22S03.10.1029/2006GL027072

Landry, MR.; Postel, JR.; Peterson, WK.; Newman, J. Broad-scale distributional patterns of hydrographic variables on the Washington shelf. In: Landry, MR.; Hickey, BM., editors. Coastal Oceanography of Washington and Oregon. Elsevier; Amsterdam, The Netherlands: 1989. p. 1-40.

Large WG, Pond S. Open ocean momentum flux measurements in moderate to strong winds. J Phys Oceanogr 1981;11:324–336.

Lentz SJ. Sensitivity of the inner-shelf circulation to the form of the eddy viscosity profile. J Phys Oceanogr 1995;25:19–28.

Lessard, EJ.; Frame, ER. The influence of the Columbia River plume on patterns of phytoplankton growth, grazing and chlorophyll on the Washington and Oregon coasts. Paper presented at Ocean Sciences Meeting, American Society of Limnology, American Geophysical Union, The Oceanography Society and Estuarine Research Foundation; Orlando, FL. 2–7 March; 2008.

Lohan MC, Bruland KW. Elevated Fe(II) and dissolved Fe in hypoxic shelf waters off Oregon and Washington: an enhanced source of iron to coastal upwelling regimes. Environ Sci Technol 2008;42:6462–6468. [PubMed: 18800515]

Lynn RL, Simpson JJ. The California Current system: the seasonal variability of its physical characteristics. J Geophys Res 1987;92:12947–12966.

MacFadyen A, Hickey BM, Foreman MGG. Transport of surface waters from the Juan de Fuca eddy region to the Washington coast. Cont Shelf Res 2005;25(16):2008–2021.

MacFadyen A, Hickey BM, Cochlan W. Influences of the Juan de Fuca Eddy on circulation, nutrients, and phytoplankton production in the northern California Current System. J Geophys Res 2008;113:C08008.10.1029/2007JC004412

McManus, DA. Bottom topography and sediment texture near the Columbia River mouth. In: Pruter, AT.; Alverson, DL., editors. The Columbia River Estuary and Adjacent Ocean Waters. University of Washington Press; Seattle, WA: 1972. p. 241-253.

Middelburg JJ, Soetaert K, Herman PMJ, Heip CHR. Denitrification in marine sediments: A model study. Global Biogeochem Cycles 1996;10:661–673.

Monteiro PMS, van der Plas A, Morholz V, Pascall A, Joubert W. Variability of natural hypoxia and methane in a coastal upwelling system: Oceanic physics or shelf biology? Geophys Res Letts 2006;33:L16614.10.1029/2006GL026234

Naqvi, SWA.; Naik, H.; Jayakumar, DA.; Shailaja, MS.; Narvekar, PV. Seasonal oxygen deficiency over the western continental shelf of India. In: Neretin, LN., editor. Past and Present Water Column Anoxia. Springer; Dordrecht, The Netherlands: 2006. p. 195-224.

Nittrouer, CA. PhD thesis. University of Washington; Seattle, Wash: 1978. The process of detrital sediment accumulation in a continental shelf environment: an examination of the Washington Shelf; p. 243

Perry, MJ.; Bolger, JP.; English, DC. Primary production in Washington coastal waters. In: Landry, MR.; Hickey, BM., editors. Coastal Oceanography of Washington and Oregon. Elsevier; Amsterdam, The Netherlands: 1989. p. 117-138.

Pauly D, Christensen V. Primary production required to sustain global fisheries. Nature 1995;374:255–257.

Pierce SD, Barth JA, Thomas RE, Fleischer GW. Anomalously warm July 2005 in the northern California Current: Historical context and the significance of cumulative wind stress. Geophys Res Letts 2006;33:L22S04.10.1029/2006GL027149

Rabalais NN, Turner RE, Sen Gupta BK, Boesch DF, Chapman P, Murrell MC. Hypoxia in the northern Gulf of Mexico: Does the science support the plan to reduce, mitigate, and control hypoxia? Estuaries Coasts 2007;30:753–772.

Ricker WE. Computation and uses of central trend lines. Can J Zool 1984;62:1897–1905.

Robinson C, Serret O, Tilstone G, Teira E, Zubkov MV, Rees AP, Woodward EMS. Plankton respiration in the Eastern Atlantic Ocean. Deep Sea Res I 2002;49:787–813.

Rowe GT, Chapman P. Continental shelf hypoxia: some nagging questions. Gulf Mex Sci 2002;20:153–160.

Ryther JH. Photosynthesis and fish production in the sea. Science 1969;166:72–76. [PubMed: 5817762]

Schwing FB, Mendelssohn R. Increased coastal upwelling in the California Current System. J Geophys Res 1997;102(C2):3421–3438.

Schwing FB, Bond NA, Bograd SJ, Mitchell T, Alexander MA, Mantua N. Delayed coastal upwelling along the U.S. West Coast in 2005: A historical perspective. Geophys Res Letts 2006;33:L22S01.10.1029/2006GL026911

Schwing, FB.; O'Farrell, M.; Steger, JM.; Baltz, K. NOAA Tech Memo NOAA-TM-NMFS-SWFSC-231. US Department of Commerce; Washington D. C: 1996. Coastal upwelling indices, West Coast of North America, 1946–1995; p. 144

Smith, P.; Bogren, K. Determination of nitrate and/or nitrite in brackish or seawater by flow injection analysis colorimeter: QuickChem Method 31-107-04-1-E. Lachat Instruments; Milwaukee, Wis: 2001. p. 12

Smith, RL. A comparison of the structure and variability of the flow field in three coastal upwelling regions: Oregon, Northwest Africa, and Peru. In: Richards, FA., editor. Coastal Upwelling. American Geophysical Union; Washington, D. C: 1981. p. 107-118.

Strub PT, Allen JS, Huyer A, Smith RL. Large-scale structure of the spring transition in the coastal ocean over western North America. J Geophys Res 1987;92(C2):1527–1544.

Sverdrup, HU.; Johnson, MW.; Fleming, RH. The Oceans, Their Physics, Chemistry, and General Biology. Prentice-Hall; New York: 1942. p. 1087http://ark.cdlib.org/ark:/13030/kt167nb66r/

Thomas AC, Brickley P. Satellite measurements of chlorophyll distribution during spring 2005 in the California Current. Geophys Res Lett 2006;33:L22S05.10.1029/2006GL026588

Walsh JJ. A carbon budget for overfishing off Peru. Nature 1981;290:300–304.

Ware DM, Thomson RE. Bottom-up ecosystem trophic dynamics determine fish production in the northeast Pacific. Science 2005;308:1280–1284. [PubMed: 15845876]

Welschmeyer NA. Fluorometric analysis of chlorophyll a in the presence of chlorophyll b and pheopigments. Limnol Oceanogr 1994;39:1985–1992.

Whitney FA, Freeland HJ, Robert M. Persistently declining oxygen levels in the interior waters of the eastern subarctic Pacific. Prog Oceanogr 2007;75:179–199.

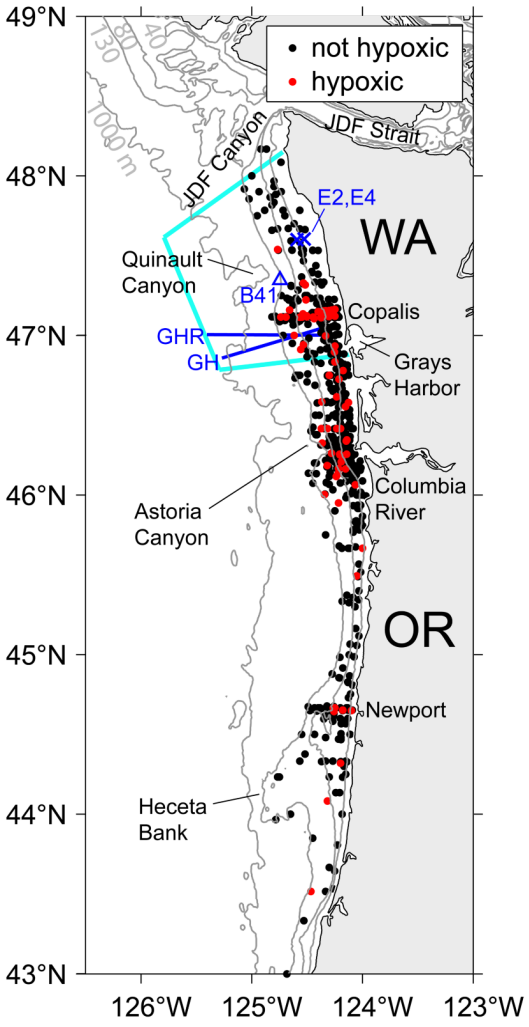

Figure 1.

Bathymetry of the Washington (WA) and Oregon (OR) continental shelf region. The 40, 80, 130, and 1000 m isobaths are shown. The blue triangle indicates the location of NDBC wind buoy 46041 (B41). The blue x's indicate locations of the E2 and E4 moorings. The GH and GHR hydrographic lines are shown as solid blue lines. Light blue lines enclose the study region on the Washington shelf. Also shown are the locations of historical near-bottom (10 m from bottom or less, 130 m bottom depth or less) stations for the Washington and Oregon continental shelves. Historical observations of near-bottom hypoxia are red; all others black.

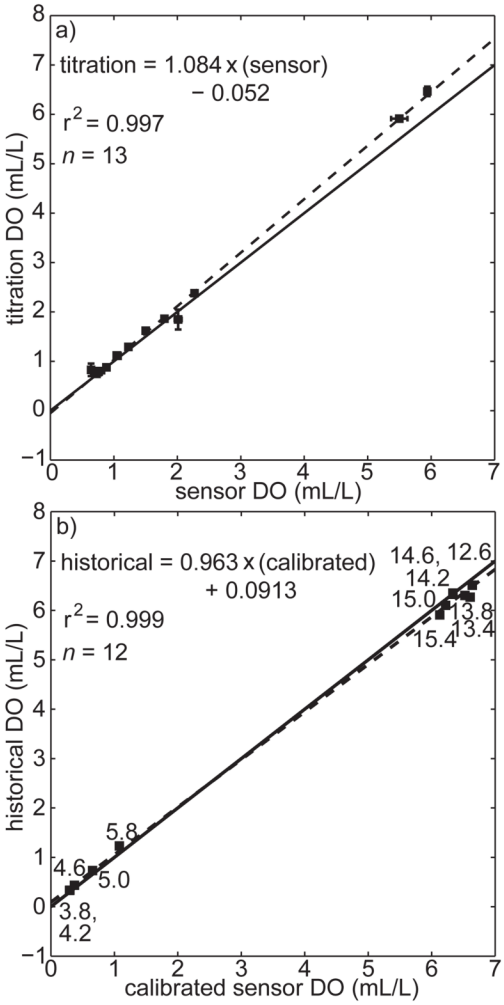

Figure 2.

a) Least-squares linear regression (dashed line) between DO concentrations measured by factory calibrated SBE 43 sensor (x-axis) and Winkler titration (y-axis) during the EH6 cruise in September 2006. Error bars, where visible, are standard deviations from triplicate samples. b) Regression between mean DO at selected temperatures from the calibrated sensor during the EH6 cruise and the historical data set, as described in the text. Numbers beside points are the center of the temperature bins. Solid lines designate 1:1 slope.

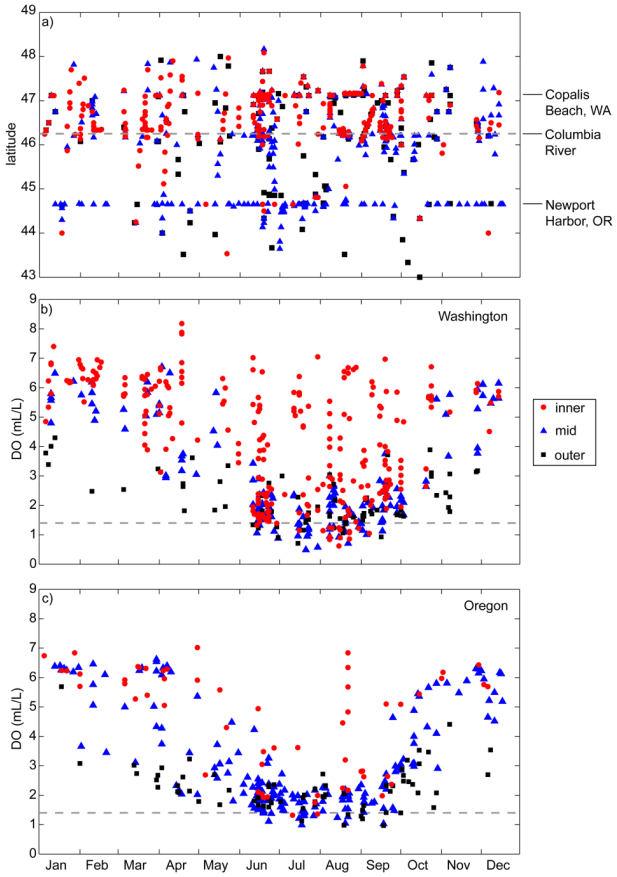

Figure 3.

a) Seasonal distribution of near-bottom DO measurements by latitude. Data are divided into three depth categories: inner shelf 0–40 m (red circles), midshelf 40–80 m (blue triangles), and outer shelf 80–130 m (black squares). The dashed lines indicate the division between Washington and Oregon data. b) Seasonal cycle of historical near-bottom DO over the Washington shelf. Symbols as in a. Dashed line indicates the 1.4 mL/L definition of hypoxia. c) Seasonal cycle of historical near-bottom DO over the Oregon shelf, as in b.

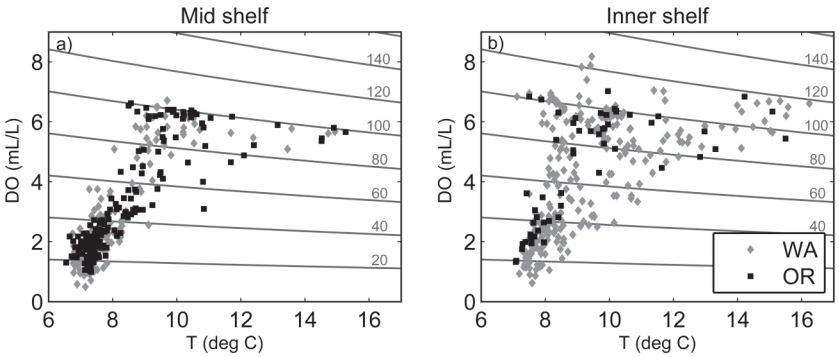

Figure 4.

Temperature vs. DO for near-bottom measurements over a) the midshelf (40–80 m bottom depth), and b) the inner shelf (40 m bottom depth or less) of Washington (grey diamonds) and Oregon (black squares). Contours indicate percent saturation at 33 psu.

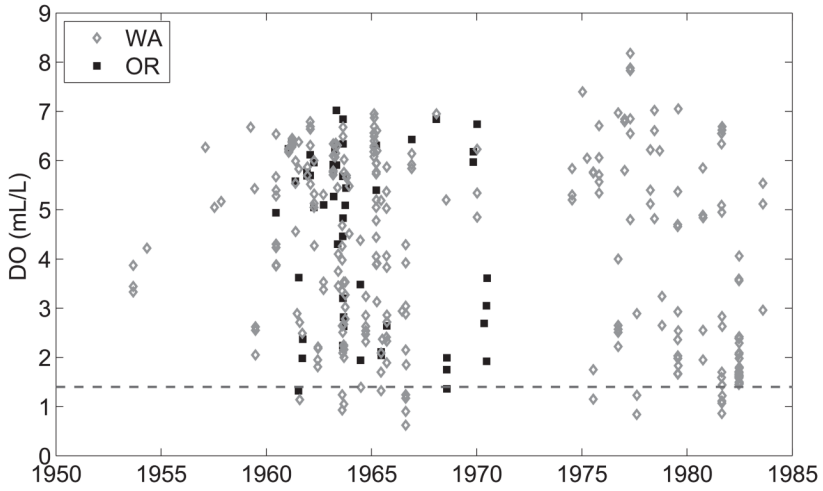

Figure 5.
Near-bottom, inner shelf (10 m from bottom or less, 40 m bottom depth or less) DO measurements for Washington (grey diamonds) and Oregon (black squares). The 1.4 mL/L definition of hypoxia is indicated by a horizontal dashed line.

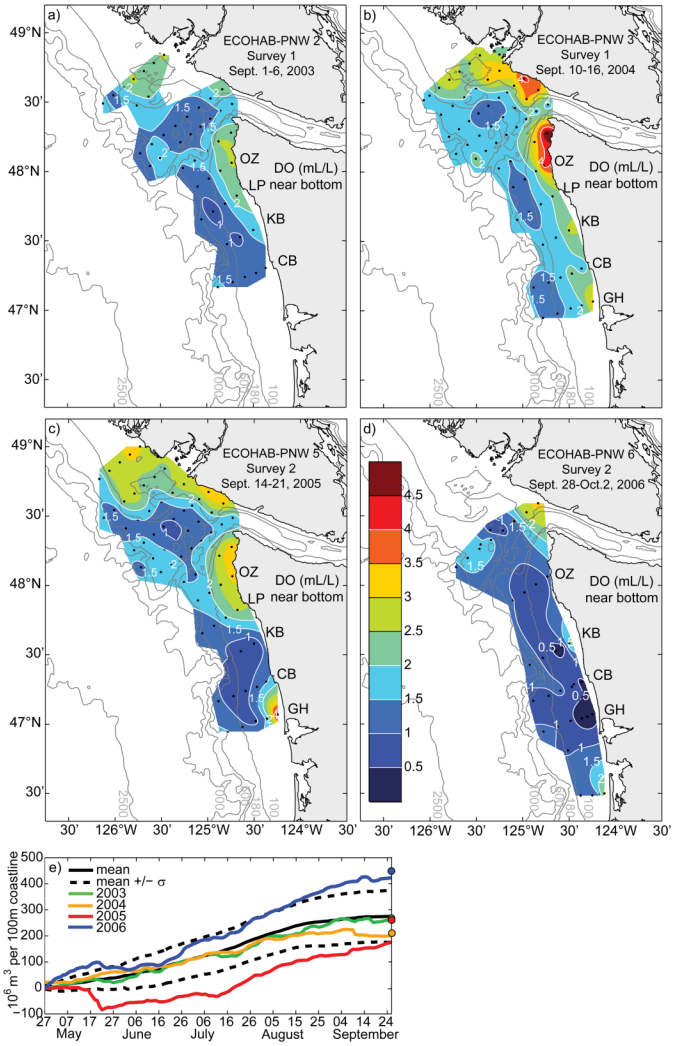

Figure 6.

Near-bottom dissolved oxygen during late summer/early fall from four different years: a) 2003, b) 2004, c) 2005, and d) 2006. DO contours, shown in the color bar in d), represent increments of 0.5 mL/L. Isobaths are indicated by grey contour lines. Station locations are shown as black dots. Abbreviations of selected transect names are shown along the Washington coast. e) Cumulative upwelling index (CUI) for the years 2003 (green), 2004 (gold), 2005 (red) and 2006 (blue). The curves show the CUI integrated from the start of the climatological upwelling season. Solid dots on the right side indicate the CUI that is obtained by integrating from the spring minimum to 26 September. The mean CUI for the years 1967–2006 is shown in solid black. The mean CUI +/− one standard deviation (σ) are shown in dashed black.

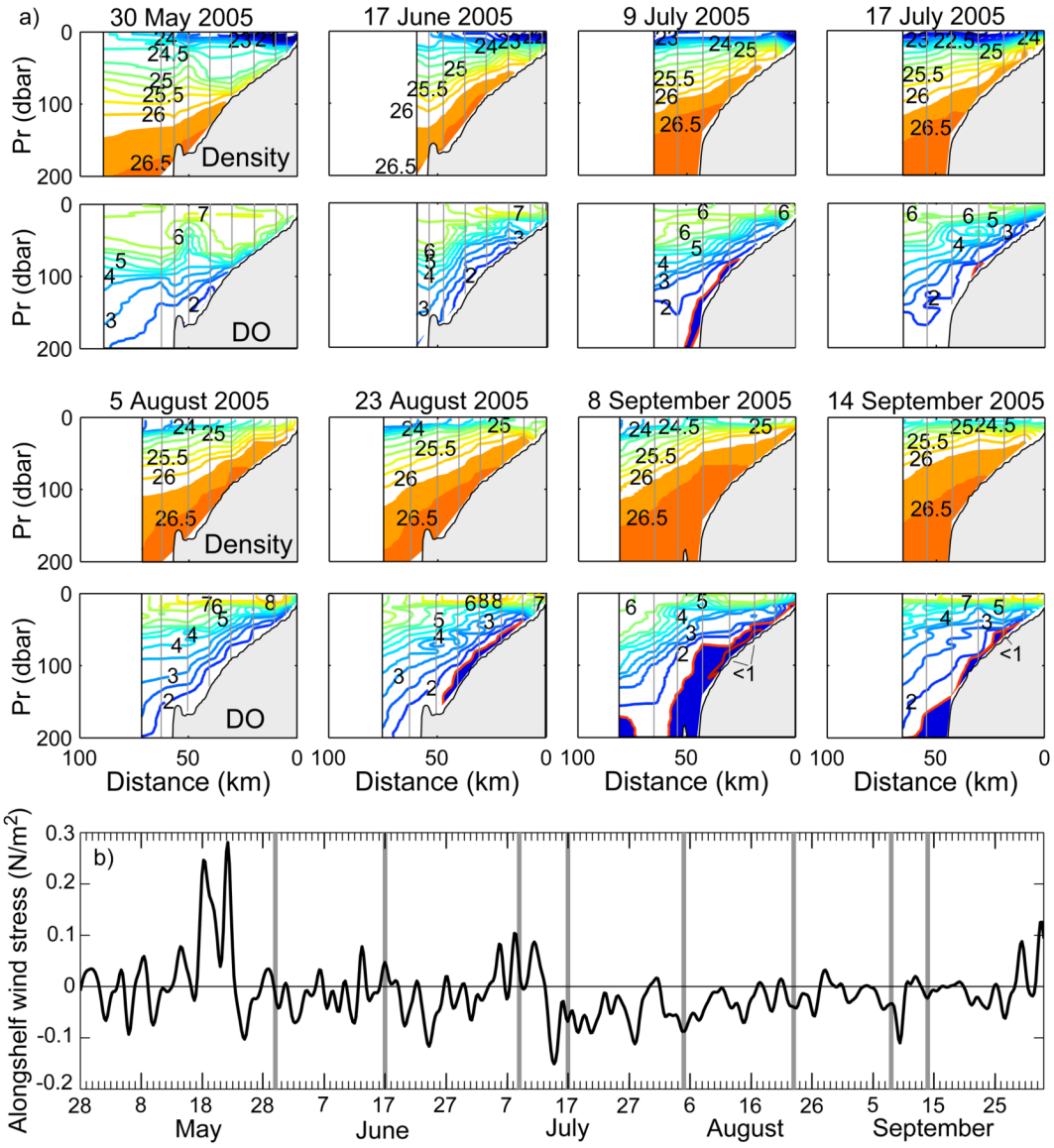

Figure 7.

a) Seasonal progression of density(first and third row) and DO (second and fourth row) off Grays Harbor during late May–mid September 2005. Grey vertical lines indicate cast locations. Contour intervals are 0.25 kg/m^3 and 0.5 mL/L. The 1.5 mL/L and 1.0 mL/L DO contours are highlighted in red; DO concentrations below 1.5 mL/L are shaded in dark blue. b) Wind stress at NDBC Cape Elizabeth buoy 46041 during mid May through late September 2005. Downwelling favorable wind stress is plotted as positive; upwelling favorable wind stress is negative. Grey vertical lines indicate the timing of sections.

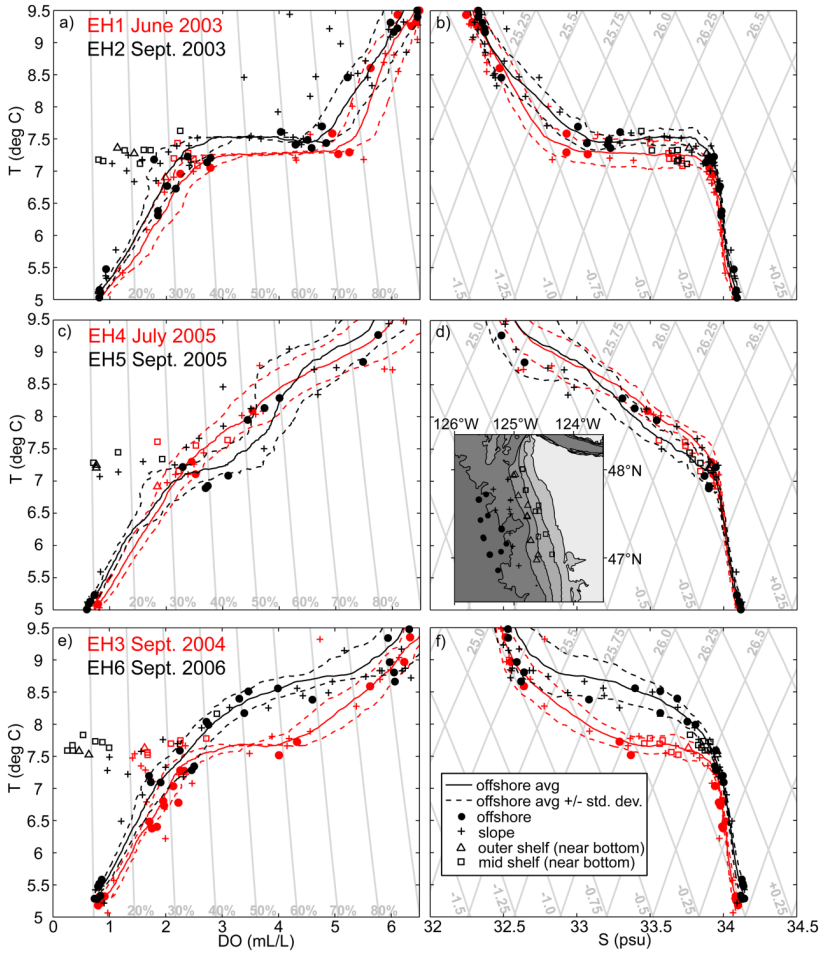

Figure 8.

Temperature vs. DO (a,c) and temperature vs. salinity (b,d) for six different cruises over the Washington shelf: June 2003 (a,b–red), September 2003 (a,b–black), July 2005 (c,d–red), September 2005 (c,d–black), September 2004 (e,f–red) and September 2006 (e,f–black). Solid and dashed lines represent a mean profile +/− the standard deviation of DO (a,c) and T (b,d) at >1000m bottom depth. Circles and crosses represent discrete values at standard depths (50, 100, 200, 500 m) at offshore (>1000 m bottom depth) and slope (130–1000 m bottom depth) stations. Triangles and squares represent discrete near-bottom values at outer and midshelf stations. Contours in a and c represent percent saturation. Contours in b and d represent σ_t and spice. Inset map in d shows station locations for discrete samples used from ECOHAB-PNW cruises 1–6.

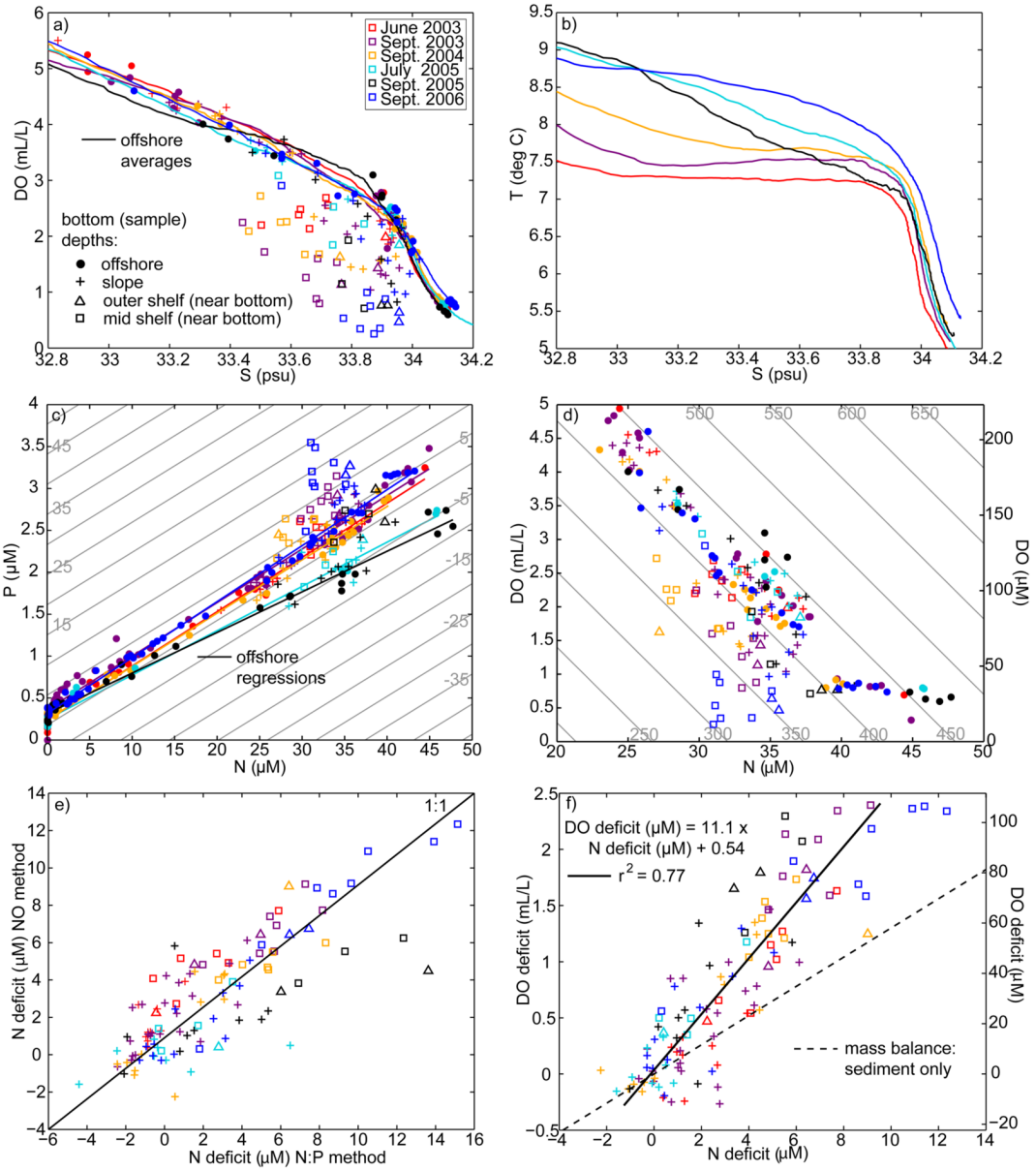

Figure 9.

a) Salinity and DO for offshore water, slope (100–200 m) water, and near-bottom shelf water. Symbols represent same range of bottom depths as Fig. 8. Solid lines indicate mean offshore profiles and colors represent different cruises. DO deficits are the vertical distance between discrete points and the mean offshore profile. b) Average offshore T and S relationships, same colors as in panel a. c) N and P, same colors and symbols as in panel a. Solid lines are linear regressions from offshore samples. Background contours represent constant -N*. N deficits are approximately equal to the distance across these contours between discrete points and the offshore regression. d) N and DO, same colors and symbols. Background contours represent constant NO. e) N deficit as calculated from the quantity NO compared with an alternate calculation based on N and P. f) Regression of DO and N deficits for slope source water and near-bottom shelf water.

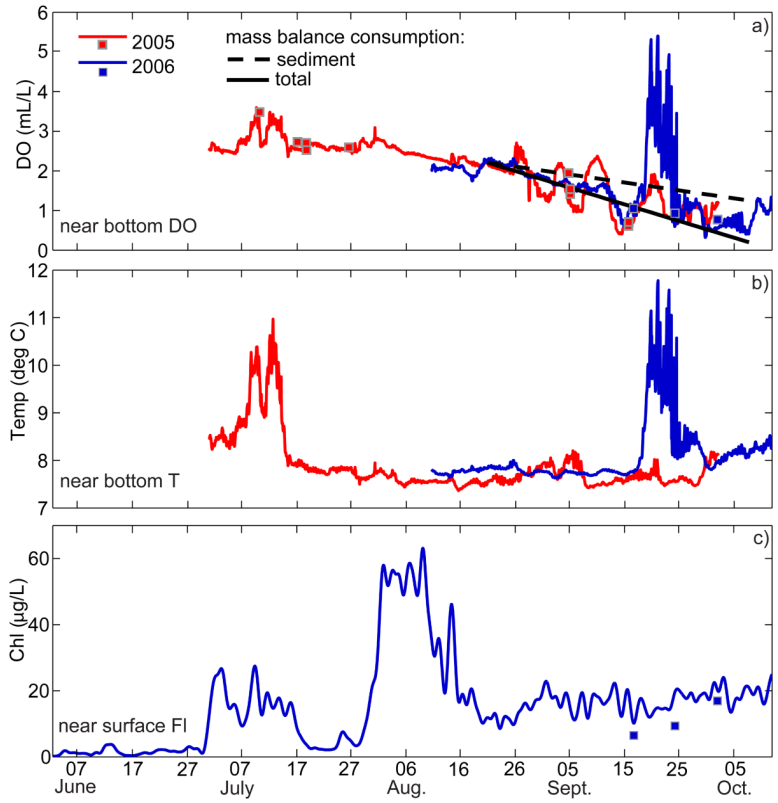

Figure 10.

Hourly time series of near-bottom DO (a) and temperature (b) at the E4 mooring location for 2005 (red lines) and 2006 (blue lines). Near-bottom DO concentrations from shipboard profiles are shown as squares. Dashed black line represents consumption of DO due to sediment demand calculated in Section 4.2 d; solid black line represents total DO consumption. c) Near surface fluorescence at the E2 mooring for 2006. Chl *a* concentrations from bottle samples are shown as squares.

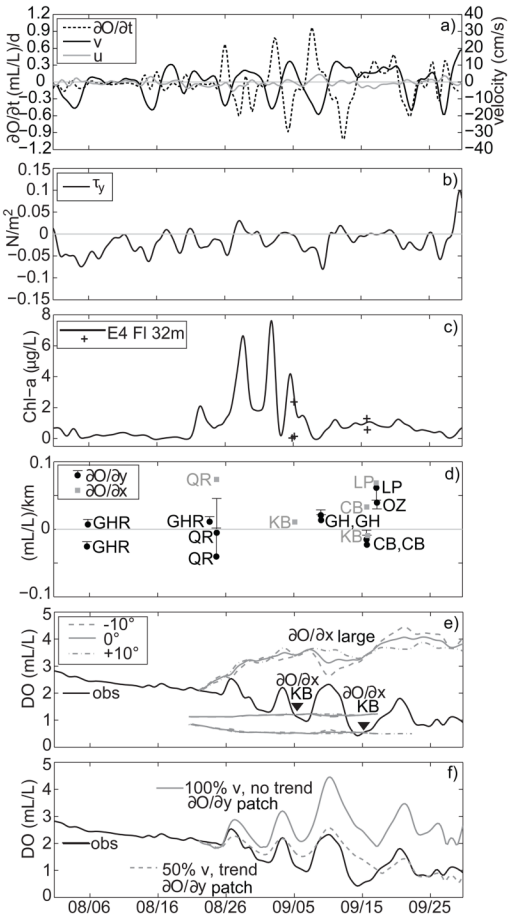

Figure 11.

Time series during the period 31 July 2005 to 29 September 2005. a) Near-bottom DO time derivative and *u*, *v* velocity components 12m above bottom at E4. b) Wind stress at NDBC Cape Elizabeth buoy 46041. c) Near-bottom fluorescence at E4, with near-bottom values from shipboard fluorescence profiles (crosses). d) DO spatial gradients in the *x*, *y* (grey, black) direction, with estimated error, E (see text, Section 2.4). e) Measured DO (black) compared to that predicted (grey) by both spatially variable gradients from the KB line, and a large constant cross-shelf gradient, with measured u. The dash-dot and dashed lines utilize velocity coordinate systems rotated ±10°. f) Measured DO time series (black) compared to that predicted (grey) by a constant along-shelf gradient on both sides of a patch with measured *v*. Dashed line includes total respiration calculated from the mass balance in Section 4.2 d, and the velocity reduced by 50% to account for bottom friction.

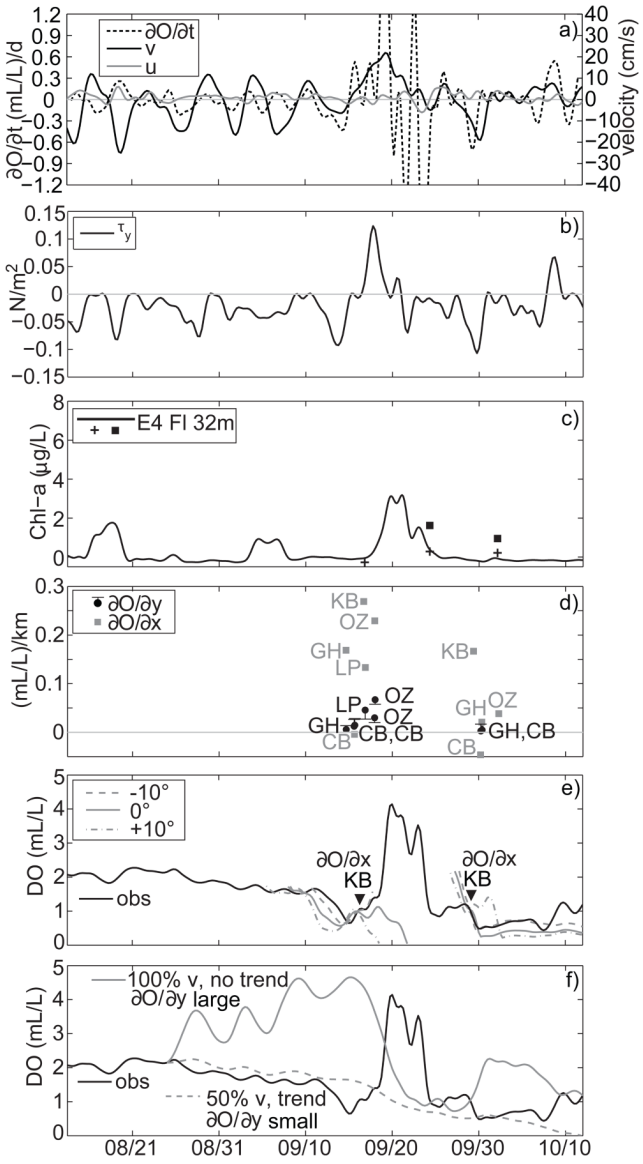

Figure 12.

Time series during the period 13 August 2006 through 12 October 2006. a) Near-bottom DO time derivative and *u*, *v* velocity components 12m above bottom at E4. b) Wind stress at NDBC Cape Elizabeth buoy 46041. c) Near-bottom fluorescence at E4,with near-bottom values from shipboard fluorescence profiles (crosses) and Chl *a* bottle samples (squares). d) DO spatial gradients in the *x*, *y* (grey, black) direction, with estimated error, E. e) Measured DO (black) compared to that predicted (grey) by both spatially variable gradients from the KB line with measured u. The dash-dot and dashed lines utilize velocity coordinate systems rotated ±10°. f) Measured DO time series (black) compared to that predicted (grey) by a constant along-shelf gradient and measured *v*. Solid line uses a large positive gradient. Dashed line uses a smaller gradient, includes total respiration calculated from the mass balance in Section 4.2 d, and velocity reduced by 50% to account for bottom friction.

Table 1

Summary of ECOHAB-PNW (EH) and RISE (R) shipboard data from 2003–2006.

Study	Cruise ID	Ship	Start	Finish
EH1	W0306A	R/V Wecoma	2 June 2003	23 June 2003
EH2	W0308C	R/V Wecoma	30 Aug. 2003	19 Sept. 2003
EH3	AT11-17	R/V Atlantis	8 Sept. 2004	28 Sept. 2004
R2-W	W0505C	R/V Wecoma	29 May 2005	21 June 2005
EH4	AT11-30	R/V Atlantis	7 July 2005	27 July 2005
R3-W	W0508C	R/V Wecoma	4 Aug. 2005	27 Aug. 2005
EH5	TUIM14VM	R/V Melville	2 Sept. 2005	22 Sept. 2005
EH6	TN200	R/V Thompson	11 Sept. 2006	4 Oct. 2006

Table 2

Mean values ± 95% confidence intervals for parameters in Equation 8. Number of samples is given by n_s.

Parameter	Value	n_s
h_{BML}*	11.8 ± 0.9 m	155
d(DO deficit)/d(N deficit)*	11.1 ± 0.9	114
f_{sed}^{DO}	−0.236 ± 0.050 (mL/L) m d^{-1} (−10.54 ± 2.25 mmol m^{-2} d^{-1})	13
$f_{sed}^{NO_3^-}$	−1.33 ± 0.11 mmol m^{-2} d^{-1}	13
$f_{sed}^{NH_4^+}$	0.48 ± 0.21 mmol m^{-2} d^{-1}	13
$f_{sed}^{NO_2^-}$	0.07 ± 0.06 mmol m^{-2} d^{-1}	13

(*)represent data from this study; flux data are from upper 200m in Devol and Christensen [1993].